

Some entanglement features of three-atoms Tavis-Cummings model: Cooperative case

M. Youssef* and A.-S. F. Obada

Department of Mathematics, Faculty of Science, Al-Azhar University, Nasr City, Cairo 11884, Egypt

N. Metwally

Department, Faculty of Science, South Valley University, Aswan, Egypt

(Dated: November 30, 2018)

In this paper we consider a system of identical three two-level atoms interacting at resonance with a single-mode of the quantized field in a lossless cavity. The initial cavity field is prepared in the coherent state while the atoms are taken initially to be either in the uppermost excited state $|eee\rangle$ or The GHZ-state or the W-state. For this system we investigate different kinds of atomic inversion and entanglement, which arise between the different parts of the system due to the interaction. Also the relationship, between entanglement and some other nonclassical effects in the statistical properties, such as collapses and revivals in the atomic inversion where superharmonic effects appear, is discussed. The Q -functions for different cases are discussed. Most remarkably it is found that the GHZ-state is more robust against energy losses, showing almost coherent trapping and Schrödinger-cat states can not be produced from such state. Also the entanglement of GHZ-state is more robust than the W-state. Another interesting feature found is that the state which has no pairwise entanglement initially will have a much improvement of such pairwise entanglement through the evolution. Sudden death and sudden revival of atoms-pairwise entanglement are produced with the W-state.

PACS numbers: 37.30.+i, 03.67.*

INTRODUCTION

The quantum entanglement phenomenon is not only one of the most interesting features of the quantum theory [1], that signifies it from the classical theory, but also lies at the heart of the new rapidly developing area known as the quantum information processing [2]. It is one of the crucial resources required in the applications in this new area of science, which include, quantum computation[3], quantum teleportation [4], quantum dense coding [5] and quantum cryptography [6]. In quantum optics domain, the interaction of an atom with a quantized electromagnetic field mode described by the Jayens-Cumming model[7, 8]leads to an entanglement of these two systems such that the total state vector cannot be written as a product of the time-dependent atomic and field component vectors [9, 10, 11]. To quantify entangled states, one should know whether they are pure or mixed states. Thus, if the entangled state is in a pure state, then it is sufficient to use von Neumann entropy as a measure of entanglement. Many efforts have been devoted to quantify entanglement, particularly for mixed states of a bipartite system, and a number of measures have been proposed, such as entanglement of formation, relative entropy of entanglement and negativity. The Peres-Horodecki criterion for separability [12, 13] leads to a natural computable measure of entanglement, called negativity [14, 15, 16]. It has been proved that the negativity $\mathcal{N}(\rho)$ is an entanglement monotone and therefore can be used as a good measure of entanglement [16].

On the other hand the cooperative nature of the interaction of a quantized radiation field with a system of two-level atoms has first been treated by Dicke [17]. A particular case of the Dicke model, when the atoms interact with a single-mode radiation field inside a cavity was investigated by Tavis and Cummings TCM [18, 19]. The interaction between a field and an ensemble of atoms develop correlations between the field and the atomic systems and between the atomic systems parties as well in the course of their dynamics. Quantifying this quantum correlations(entanglement) is one of the open problems. Multi-qubit systems are of interest to be investigated both theoretically and experimentally. In recent years, great achievements have been made in the application of three-qubit states, because understanding of entanglement and dynamics of three-qubit system is an important matter, for example, it has many applications in quantum cryptography [20], quantum computation [21] and quantum gates [22, 23].

In this paper, we consider a system of identical three two-level atoms interacting at resonance with a single-mode of the quantized field in a lossless cavity. The initial cavity field is prepared in the coherent state while the atoms may assume different initial states. For this system, we investigate some kinds of entanglement which arise between the different parts of the system due to the interaction. We use the concurrence, the generalized I-concurrence and the negativity to quantify entanglement between different parties as well as the

3-particle residual entanglement. Also we look at the relationship between this entanglement and some other nonclassical effects in the statistical properties such as collapses and revivals in the atomic inversion. The field dynamics and atoms-field entanglement are discussed through Q -function.

This paper is organized as follows. In section 2 we introduce the system and its solution. Section 3 is devoted to the atomic inversions. In section 4 we study the field atom entanglement, two-atom entangle and the atomic system purity. Section 5 is devoted to the residual 3-particle entanglement. The field dynamics in phase space, the possibility of having a cat state and the atoms-field entanglement are addressed in section 6. Finally in section 7. we conclude the paper with a discussion of the results.

THE MODEL AND ITS TIME EVOLUTION

We consider a system of three identical two-level atoms interacting with a quantized single-mode electromagnetic field. Under the rotating-wave approximation and resonant condition, the Hamiltonian of this system reads:

$$\begin{aligned} \hat{H} = \hat{H}_0 + \hat{H}_I = \omega_f \left(\hat{a}^\dagger \hat{a} + \frac{1}{2} \sum_{i=a,b,c} \hat{\sigma}_z^{(i)} \right) \\ + g \left(\hat{a} \sum_{i=a,b,c} \hat{\sigma}_+^{(i)} + \hat{a}^\dagger \sum_{i=a,b,c} \hat{\sigma}_-^{(i)} \right) \end{aligned} \quad (1)$$

where ($\hbar = 1$). The terms \hat{H}_0 and \hat{H}_I represent the free and interaction hamiltonians respectively; ω_f is the field frequency, and equals the atomic transition frequency on resonance; $\hat{\sigma}_+^{(i)}$, $\hat{\sigma}_-^{(i)}$ and $\hat{\sigma}_z^{(i)}$ are the the usual raising, lowering and inversion operators for the i^{th} atom, satisfying $[\hat{\sigma}_+^{(i)}, \hat{\sigma}_-^{(i)}] = \hat{\sigma}_z^{(i)}$, $[\hat{\sigma}_z^{(i)}, \hat{\sigma}_\pm^{(i)}] = \pm 2\hat{\sigma}_\pm^{(i)}$, $[\hat{\sigma}_\mu^{(i)}, \hat{\sigma}_\nu^{(j)}] = 0$ while $\hat{a}^\dagger(\hat{a})$ is the Bose creation (annihilation) operator for the quantized field mode satisfying the commutation relations $[\hat{a}, \hat{a}^\dagger] = 1$, and g is the coupling constant. Since $[\hat{H}_0, \hat{H}_I] = 0$, it follows that, the Hamiltonian (1) conserves the total number of excitations N , i.e. the total excitation operator

$$\hat{N} = \hat{a}^\dagger \hat{a} + \frac{1}{2} \sum_{i=a,b,c} \hat{\sigma}_z^{(i)} \quad (2)$$

is a constant of motion. This provides a decomposition for the system Hilbert space as $\mathcal{H} = \sum_{n=0}^{\infty} \oplus \mathcal{H}_n$ such that, $\mathcal{H}_0 = \{|g, g, g; 0\rangle\}$, $\mathcal{H}_1 = \{|g, g, g; 1\rangle, |g, e, g; 0\rangle, |g, g, e; 0\rangle, |e, g, g; 0\rangle\}$ and $\mathcal{H}_2 = \{|g, g, g; 2\rangle, |e, g, g; 1\rangle, |g, e, g; 1\rangle, |g, g, e; 1\rangle, |e, e, g; 0\rangle, |e, g, e; 0\rangle, |g, e, e; 0\rangle\}$ are a one-dimensional, 4-dimensional and 7-dimensional eigensubspaces of N and

$\mathcal{H}_{n+3}|_{n=0}^{\infty} = \{|eee; n\rangle, |eeg; n+1\rangle, |ege; n+1\rangle, |gee; n+1\rangle, |egg; n+2\rangle, |geg; n+2\rangle, |gge; n+2\rangle, |ggg; n+3\rangle\}$

are the eight-dimensional eigensubspaces of N . In the Hilbert space constituted by the above basis, the interaction \hat{H}_I is a diagonal blocks matrix made up of 8×8 sub-matrices, every sub-matrix represents a subspace corresponding to a definite excitation number N . However we found that it is more appropriate for this system to use the Dicke states [17] as a basis, because of the degeneracy produced by the symmetry. For N spin-1/2 particle system, the Dicke states are defined as the states $|S, m_s\rangle$ that are common eigenstates of both the square of the total spin operator \hat{S}^2 and its component along z -axis "the quantization axis" \hat{S}_z with the corresponding eigenvalues $S(S+1)\hbar$ and $m_s\hbar$. For our system the Dicke states in terms of the above mentioned product states are given by

$$\begin{aligned} |\mathcal{D}_1\rangle &= |eee; n\rangle \\ |\mathcal{D}_2\rangle &= \frac{1}{\sqrt{3}} (|eeg; n+1\rangle + |ege; n+1\rangle + |gee; n+1\rangle) \\ |\mathcal{D}_3\rangle &= \frac{1}{\sqrt{3}} (|egg; n+2\rangle + |geg; n+2\rangle + |gge; n+2\rangle) \\ |\mathcal{D}_4\rangle &= |ggg; n+3\rangle \\ |\mathcal{D}_5\rangle &= \frac{1}{\sqrt{6}} (2|gee; n+1\rangle - |ege; n+1\rangle - |eeg; n+1\rangle) \\ |\mathcal{D}_6\rangle &= \frac{1}{\sqrt{2}} (|eeg; n+1\rangle - |ege; n+1\rangle) \\ |\mathcal{D}_7\rangle &= \frac{1}{\sqrt{6}} (|geg; n+2\rangle + |gge; n+2\rangle - 2|egg; n+2\rangle) \\ |\mathcal{D}_8\rangle &= \frac{1}{\sqrt{2}} (|gge; n+2\rangle - |geg; n+2\rangle) \end{aligned} \quad (3)$$

The first four states are fully symmetric with respect to the permutation of particles, while the other four states are in fact a two state of mixed symmetry, which correspond to two degenerate representations, each of dimension 2 [24]. By substituting into the Schrödinger equation $-i \frac{d|\Psi(\tau)\rangle}{d\tau} = \hat{H}_I |\Psi(\tau)\rangle$, where $\tau = gt$, then the wave function generally can be written as $|\Psi(\tau)\rangle = \sum_{i=1}^8 X_i^{(n)}(\tau) |\mathcal{D}_i\rangle$.

We found, as expected, that the equations of the probability amplitudes which correspond to the two degenerate states are decoupled from each other and from the four amplitudes which correspond to the fully symmetric Dicke states. The initial state of the system will be taken as follows:

$$\begin{aligned} |\Psi(0)\rangle &= |\Psi_a(0)\rangle \otimes |\Psi_f(0)\rangle \\ |\Psi_a(0)\rangle &= C_e |e, e, e\rangle + \frac{1}{\sqrt{3}} C_{w1} (|e, e, g\rangle + |e, g, e\rangle + |g, e, e\rangle) \\ &\quad + \frac{1}{\sqrt{3}} C_{w2} (|g, g, e\rangle + |g, e, g\rangle + |e, g, g\rangle) + C_g |g, g, g\rangle \\ |\Psi_f(0)\rangle &= \sum_{n=0}^{\infty} q_n |n\rangle; \quad q_n = e^{(-|\alpha_0|^2/2)} \frac{\alpha_0^n}{\sqrt{n!}} \end{aligned} \quad (4)$$

where $|C_e|^2 + |C_{w1}|^2 + |C_{w2}|^2 + |C_g|^2 = 1$. For the above initial atomic states the wave function evolve only inside the subspace spanned by the fully symmetric Dicke states and the probability amplitudes of the other state vanishes, hence our system is equivalent to a four-level Dicke atom. This is a generalization to the case of two identical atoms [25], where the antisymmetric states do not participate in the dynamics. Solving the coupled four equations of the probability amplitudes we get the wave function of system at any time

$$\begin{aligned} |\Psi(\tau)\rangle &= \sum_{n=0}^{\infty} \sum_{i=1}^4 X_i^{(n)}(\tau) |\mathcal{D}_i\rangle \\ X(\tau) &= [X_1^{(n)}(\tau), X_2^{(n)}(\tau), X_3^{(n)}(\tau), X_4^{(n)}(\tau)]^T \\ &= \mathcal{U}X(0) \end{aligned} \quad (5)$$

where the evolution matrix \mathcal{U} is given by

$$\mathcal{U} = \begin{pmatrix} \mathcal{U}_{11} & \mathcal{U}_{12} & \mathcal{U}_{13} & \mathcal{U}_{14} \\ \mathcal{U}_{21} & \mathcal{U}_{22} & \mathcal{U}_{23} & \mathcal{U}_{24} \\ \mathcal{U}_{31} & \mathcal{U}_{32} & \mathcal{U}_{33} & \mathcal{U}_{34} \\ \mathcal{U}_{41} & \mathcal{U}_{42} & \mathcal{U}_{43} & \mathcal{U}_{44} \end{pmatrix} \quad (6)$$

The explicit form of the matrix elements are given in the appendix, where in there we have

$$\begin{aligned} \mu_{1,2} &= \frac{1}{2} \left(\delta \pm \sqrt{\delta^2 - 36\eta^2\gamma^2} \right) \\ \delta &= (4\beta^2 + 3\gamma^2 + 3\eta^2) \\ \gamma &= \sqrt{n+1}, \quad \beta = \sqrt{n+2}, \quad \eta = \sqrt{n+3} \end{aligned} \quad (7)$$

Note that $X_i^{(n)}$ has q_{n+i-1} as a factor, where $i=1,2,3,4$. By using this wave function, we discuss different aspects of the system in what follows.

ATOMIC INVERSIONS

Energy is the primary quantity determining the properties of physical systems. The atomic inversion and levels occupation probabilities are the simplest nontrivial physical quantities in the atom-field interaction, that display the exchange of energy between the field and the atoms. More important to our investigation, the atomic inversions display the primary nonclassical effect namely, the collapse and revival structure [26, 27, 28, 29] from which we can have information about the atoms-field entanglement and disentanglement through the dynamics [9, 10, 11, 30, 31, 32]. Finally the collapses and revivals will be clearly connected to the evolution of the Q-function [33, 34]. In this section we shall discuss these quantities. We shall deal with three quantities namely,

$$W_T(t) = \sum_{n=0}^{\infty} \left\{ |X_1^{(n)}|^2 - |X_4^{(n)}|^2 \right\} \quad (8)$$

$$\begin{aligned} W_a(t) &= \langle \Psi(t) | \hat{\sigma}_z^{(a)} | \Psi(t) \rangle = \sum_{n=0}^{\infty} \left\{ |X_1^{(n)}|^2 + \frac{1}{3} |X_2^{(n)}|^2 \right. \\ &\quad \left. - |X_4^{(n)}|^2 - \frac{1}{3} |X_3^{(n)}|^2 \right\} \end{aligned} \quad (9)$$

$$P_{ini}(t) = |\langle \Psi(0) | \Psi(t) \rangle|^2 \quad (10)$$

where, $W_T(t)$ is the total atomic inversion, $W_a(t)$ is the inversion of the atom a and $P_{ini}(t)$ is the probability of occupation of the initial state. The two-atoms inversion is double the one-atom inversion. In Fig.1 we show these quantities for the atoms being initially (a) in the excited state $|\Psi_a(0)\rangle = |eee\rangle$, or (b) the atoms initially in a GHZ-state [35], $|\Psi_a(0)\rangle = |\text{GHZ}\rangle = \frac{1}{\sqrt{2}}(|ggg\rangle + |eee\rangle)$, which has the property that tracing over any one qubit results in a maximally mixed state containing no entanglement between the remaining two qubits or (c) in genuine entangled W-state "Werner state" [36], $|\Psi_a(0)\rangle = |W\rangle = \frac{1}{\sqrt{3}}(|eeg\rangle + |ege\rangle + |gee\rangle)$, for this state when tracing over any one qubit the average remaining bipartite entanglement is maximal. Before we dwell in the discussion of the figures we present a rough analysis about the time dependent quantities in the expressions (8, 9 and 10). Since we are dealing with a coherent state for which $\bar{n} = 100$, it is well known that the effective excitation will be due to the photons within the range $|n - \bar{n}| \leq \Delta n = \sqrt{\bar{n}}$. For these photons and those within a reasonably range to them, the radicands appearing in the expressions for β , γ and η in Eq.(7) can be approximated to $\sqrt{\bar{n}}$ and the expressions for μ_1 , μ_2 are then given by "9n" and "n" respectively. Thus the Rabi frequencies appearing in the expressions for \mathcal{U}_{ij} are to be approximated as $3\sqrt{\bar{n}}$ and $\sqrt{\bar{n}}$ respectively. Keeping these points in mind, we find the following for the case of the atomic initial state $|\Psi_a(0)\rangle = |eee\rangle$, i.e., the three atoms are in their excited states: Regarding the quantity $W_T(\tau)$, the time-dependent summand is proportional to $\frac{1}{16}(\cos 6\sqrt{\bar{n}}\tau + 15 \cos 2\sqrt{\bar{n}}\tau)$, containing superharmonics which results in three revival times $\frac{2\pi}{3}\sqrt{\bar{n}}$, $\frac{4\pi}{3}\sqrt{\bar{n}}$ and $2\pi\sqrt{\bar{n}}$ related to the trigonometric functions with two equal heights for the 1st and 2nd revival and 16 times larger at the 3rd revival. This appears clearly in Fig.1.(a1). On the other hand for the single atom population inversion $W_a(t)$, the time dependent summand is proportional to $\cos 2\sqrt{\bar{n}}\tau$, which results in a single revival time at $2\pi\sqrt{\bar{n}}$ which is depicted in Fig.1.(a2). The $P_{ini}(\tau)$ has the term $\frac{1}{32}(10 + \cos 6\sqrt{\bar{n}}\tau + 6 \cos 4\sqrt{\bar{n}}\tau + 15 \cos 2\sqrt{\bar{n}}\tau)$ in its summand, composed of 2 and 3 superharmonics giving rise to revivals times at $\frac{2\pi}{3}\sqrt{\bar{n}}$, $\pi\sqrt{\bar{n}}$, $\frac{4\pi}{3}\sqrt{\bar{n}}$ and $2\pi\sqrt{\bar{n}}$. The second revival is larger than the 1st and 3rd because of the coefficients of $\cos 6\sqrt{\bar{n}}\tau$ and $\cos 4\sqrt{\bar{n}}\tau$ whiles the 4th, at $2\pi\sqrt{\bar{n}}$, is the highest as the four revivals coincide. This is shown faithfully in Fig.1.(a3) whereas the quantity P_{ini} fluctuates around $\frac{5}{16}$.

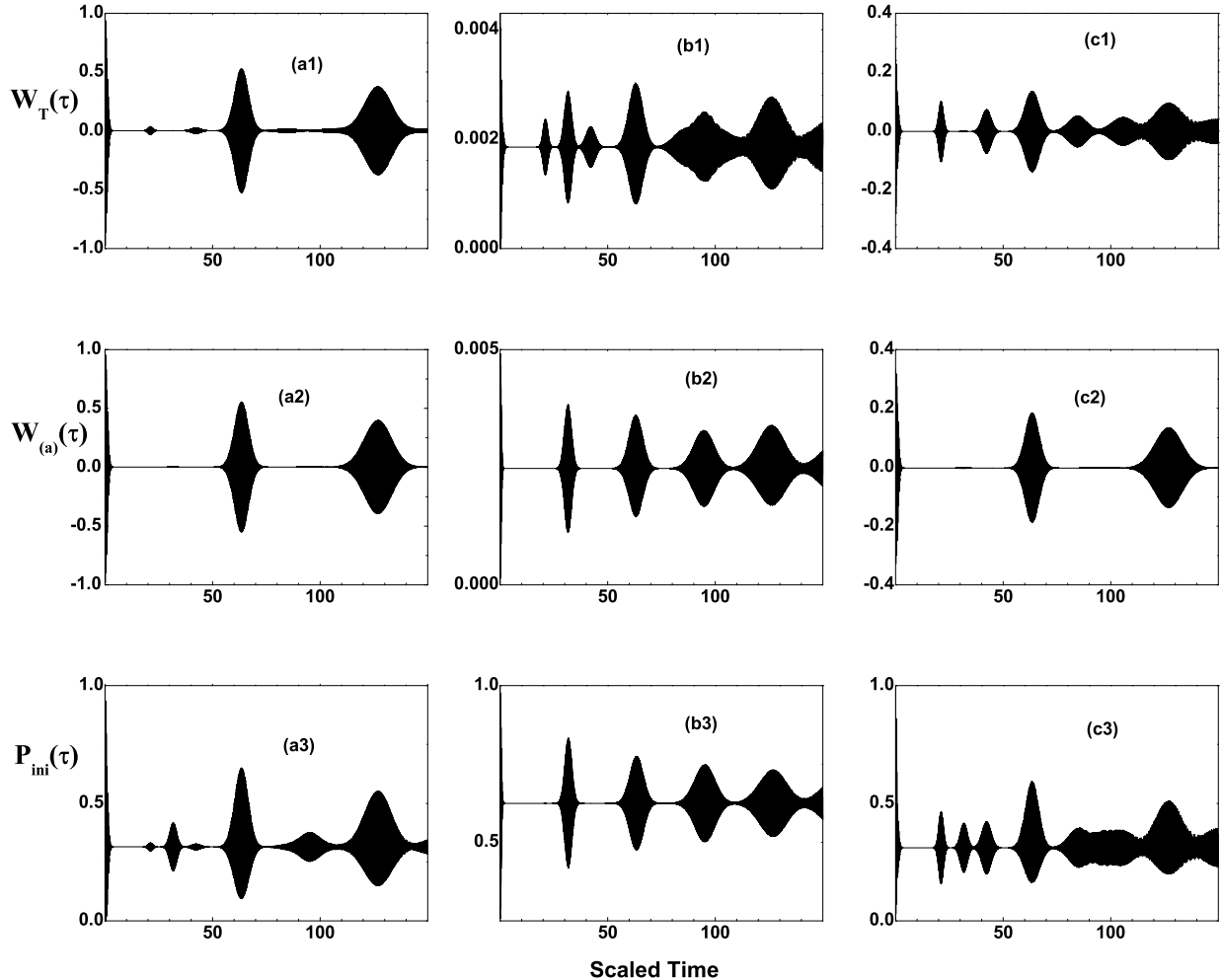


FIG. 1: Evolution of the total atomic inversions $W_T(\tau)$, single-atom inversions $W_a(\tau)$ and the initial state populations $P_{ini}(\tau)$, Eq.(??) for different initial atomic states (a) $|eee\rangle$ -initial state, (b) $|GHZ\rangle$ -initial state and (c) $|W\rangle$ -initial state. The field in a coherent state with $|\alpha|^2 = 100$

Now we look at the initial state $|\Psi_a(0)\rangle = \frac{1}{\sqrt{2}}(|ggg\rangle + |eee\rangle)$ Figs.1(1b,2b,3b), and applying the same analysis as in the previous case, we find the following:- The quantity $W_T(\tau)$ as well as $W_a(\tau)$ is almost zero as can be seen from Fig.1(b1) and Fig.1(b2). In contrast, the quantity $P_{ini}(\tau)$ depends on the summand of the form $\frac{1}{8}(5 + \cos 4\sqrt{n}\tau)$ which results in revival times $\pi\sqrt{n}$ and $2\pi\sqrt{n}$ shown clearly in Fig.1(b3). Also it exhibits the fluctuations around $\frac{5}{8}$. These results show that, starting from the GHZ-state would result in coherent trapping and the atoms almost do not interact with the field. This is shown in the value of $\frac{5}{8}$ for the probability for the atoms staying in the initial state.

The case of the atomic initial Werner state namely

$|\Psi_a(0)\rangle = \frac{1}{\sqrt{3}}(|eeg\rangle + |ege\rangle + |gee\rangle)$ is shown in Figs.1(c1,c2,c3). Analysis of the summand of $W_T(\tau)$ reveals that the time-dependence is of the form $(\cos 6\sqrt{n}\tau + \cos 2\sqrt{n}\tau)$. This amounts to the revival times $\frac{2\pi}{3}\sqrt{n}$, $\frac{4\pi}{3}\sqrt{n}$ and $2\pi\sqrt{n}$ with the amplitude at the 3rd revival twice as much as the 1st revival. Whereas the single atom population inversion has a single revival at $2\pi\sqrt{n}$ because the time dependent term in the summand is proportional to $\cos 2\sqrt{n}\tau$. It is worthnoting that the fluctuations in the population inversion are the highest for the $|eee\rangle$ initial state and the lowest for the GHZ initial state showing an almost coherent trapping [37] for the latter in such a way to resist exchange of energy with the field, whereas the W-state is in the middle, showing a modest degree of exchange of the energy with the field.

COOPERATIVE AND ATOMS-PAIRWISE ENTANGLEMENT

The system under investigation is a multipartite system initially in an over all pure state, occupying the following Hilbert space $\mathcal{H} = \mathcal{H}_a \otimes \mathcal{H}_b \otimes \mathcal{H}_c \otimes \mathcal{H}_f$ with dimension $2 \otimes 2 \otimes 2 \otimes \infty$. Since we consider here only the cooperative case, whereas the Hamiltonian is symmetric under atom exchange, thus there are only eight nonequivalent partitions of bipartite subsystems namely: (i) $f \otimes (abc)$, $(fc) \otimes ab$, $(fcb) \otimes a$, (ii) $f \otimes (ab)$, (iii) $f \otimes a$, (iv) $(fb) \otimes a$, (v) $a \otimes (bc)$ and (vi) $a \otimes b$, corresponding to the field times the whole atomic system, two-atoms times the field with the remaining atom, one-atom times the field with the other two atoms, the field times two-atoms, the field times one-atom, one atom times the field with one-atom, one-atom times the other two atoms and one-atom times one-atom respectively.

These partitions except (i), are obtained by tracing over one or more Hilbert-subspaces of the total Hilbert space and hence they are generally mixed states. For convenience and simplicity we will only study the entanglement evolution of the partitions (i) and the entanglement of the last partition, i.e. atom-atom entanglement. In the following section the entanglement of the bipartite partition (v), will be discussed together with the phenomenon of entanglement sharing [3, 38] and the residual 3-particle entanglement using the negativity.

For the bipartite partitions in (i), each one of them start from an over all pure state and a number of widely accepted measures of entanglement are available. An easier way to quantify the entanglement in this bipartite partitions is to use the square of the pure-state I-concurrence introduced in Ref. [39],

$$C^2(\Psi) = 2\nu_{d_1}\nu_{d_2}[1 - \text{Tr}\{\rho_f^2\}] = 2\nu_{d_1}\nu_{d_2}[1 - \text{Tr}\{\rho_{abc}^2\}] \quad (11)$$

This generalizes the original concurrence's notion introduced by Hill and Wootters [40] $C(\Psi) \equiv \sqrt{\langle \Psi | S_2 \otimes S_2 | \Psi \rangle \langle \Psi | \Psi \rangle} = |\langle \Psi | \sigma_y \otimes \sigma_y | \Psi^* \rangle|$ for pairs of qubits in a joint pure state $|\Psi\rangle$, to be applied for pairs of quantum systems of arbitrary dimension $d_1 \otimes d_2$ in a joint pure state. The concurrence is defined with the help of a superoperator S_2 , whose action on a qubit density operator $\rho = |\Psi\rangle\langle\Psi|$ is to flip the spin of the qubit density operator $S_2(\rho) = \rho^*$; $\rho^* = |\tilde{\Psi}\rangle\langle\tilde{\Psi}|$, where $|\tilde{\Psi}\rangle = \sigma_y \otimes \sigma_y |\Psi^*\rangle$, the asterisk denotes the complex conjugate and σ_y is the Pauli matrix. Rungta et al. [39] use the formalism for superoperators [41] to generalize the spin-flip superoperator S_2 for a qubit to a superoperator S_d that acts on qudit states (d-dimensional states). For defining an I-concurrence, one should choose the scaling factor ν_d to be independent of d , otherwise, the pure state I-concurrence could be

changed simply by adding extra, unused dimensions to one of the subsystems. To be consistent with the qubit concurrence, one should choose $\nu_d = 1$. With this choice the pure-state I-concurrence runs from zero for product states to $I_{max} = \sqrt{\frac{2(m-1)}{m}}$, where $m = \min(d_1, d_2)$, for a maximally entangled state. Henceforth we will use only the term I-concurrence when refereing to it.

On the other hand, Wootters extended the concurrence notation to the case of a two qubits in an arbitrary joint mixed state, he showed that the entanglement of formation [42, 43] of an arbitrary two-qubits mixed state ρ can be written in terms of the minimum average pure-state concurrence of ensemble decompositions of ρ , and he derived an explicit expression for this minimum in terms of the eigenvalues of $\rho\tilde{\rho}$ [44].

$$C(\rho) = \max\{0, \lambda_1 - \lambda_2 - \lambda_3 - \lambda_4\} \quad (12)$$

where λ_i 's are the eigenvalues, in decreasing order, of the Hermitian matrix $R = \sqrt{\sqrt{\rho}\tilde{\rho}\sqrt{\rho}}$. Alternatively, one can say that the λ_i 's are the square roots of the eigenvalues of the matrix $\rho\tilde{\rho}$ and each λ_i is a non-negative real number. The spin-flipped state $\tilde{\rho}$ is obtained by spin flipping, namely $\tilde{\rho} = (\sigma_y \otimes \sigma_y)\rho^*(\sigma_y \otimes \sigma_y)$. where again the asterisk denote the complex conjugate. For a pure state $|\Psi\rangle$, R has only one eigenvalue that may be nonzero, namely, $C(\Psi)$ Eq.(11). Wootters called this minimum average, the concurrence of the mixed state. The entanglement of the last partition, i.e. atom-atom entanglement can be investigated using this formula.

It is worthnoting that the remanning partitions are all in a mixed state with dimensions $2 \otimes \infty$, $4 \otimes \infty$ and $2 \otimes 4$, which can not be quantified by any of the above mentioned entanglement measures. Following Tessier et al. [3], we can quantify the entanglement for all the above partitions using Osborne's formula [45] for the I-tangle $\tau(\rho_{AB})$ for mixed states ρ_{AB} of a pair AB of qudits, of dimensions d_A and d_B , having no more than two nonzero eigenvalues, i.e., ρ_{AB} with rank no greater than 2. The I-tangle τ between A and B is given by the expression

$$\tau(\rho_{AB}) = \text{Tr}\{\rho_{AB}\tilde{\rho}_{AB}\} + 2\lambda_{min}(1 - \text{Tr}\{\rho_{AB}^2\}) \quad (13)$$

where λ_{min} is is the smallest eigenvalue of the real symmetric 3×3 matrix M as defined in [45]

In Fig.2 we show the I-concurrence of the reduced density matrices ρ_{abc} , ρ_{ab} and ρ_a , (a) for the $|eee\rangle$ case, (b) the $|GHZ\rangle$ case and (c) the $|W\rangle$ case. This type of entanglement may be called a cooperative entanglement. Figs.2(a1,a2,a3,b1,c1) begin from zero which corresponds to the initial product state while Figs.(b2,b3,c2,c3) start from 3-particle maximum entanglement state. They suddenly increase in the collapse region to reach the maximum values, $I_{max} = 1.34, 1.23$ and 1 for $f \otimes (abc)$,

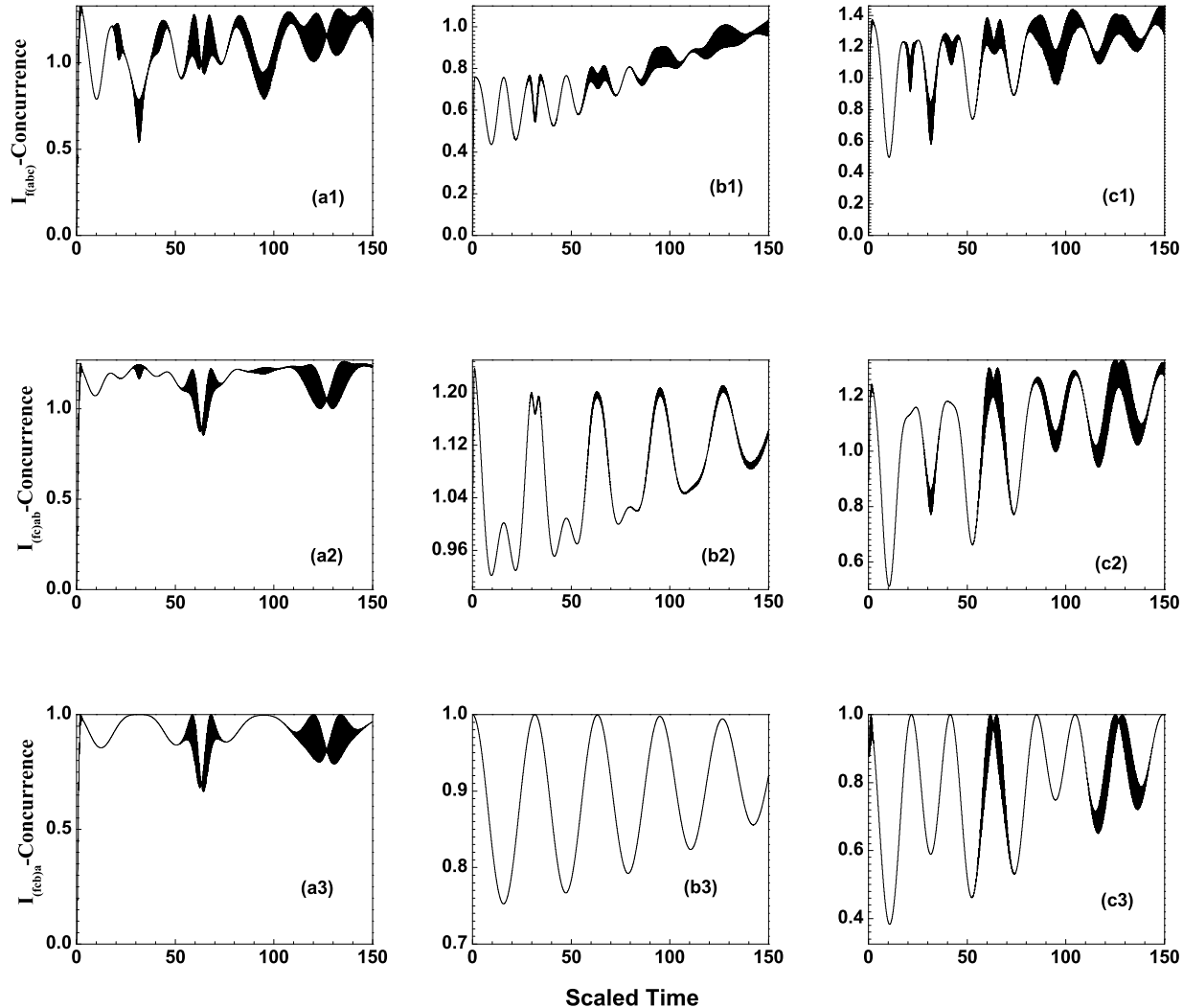


FIG. 2: The I-concurrence for the three bipartite partitions in (i), (a) $|eee\rangle$ -initial state, (b) $|GHZ\rangle$ -initial state and (c) $|W\rangle$ -initial state.

$(fc) \otimes ab$ and $(cb) \otimes a$ respectively. The exception is the entanglement between the field and the total atomic system in the case of the GHZ-state in Fig.2(b1), which did not reach this maximum. This reflects the robustness of the initial entanglement of this state, i.e., the initial entanglement between the atoms resists the interaction and the energy exchange between them and the field as shown in the discussion of the population inversion of last section. When this entanglement becomes rather weak the field-atoms entanglement increase rapidly to the maximum value I_{max} . On the other hand the W-state case did not show such robustness. There are many local minima and maxima asymptotically increasing to reach the maximum values, I_{max} . It is noticed that the GHZ-state

shows more periodicity than the other two cases. Finally, it is clear that the local maxima and minima of the $f \otimes (abc)$ and $(a) \otimes fbc$ figures are opposite to each other. Fig.3 shows the concurrence of the reduced density matrix $C(\rho_{ab})$ for the different initial states. In contrast to the above cooperative entanglement, the atom-atom entanglement asymptotically decreases and vanishes. The initially excited atoms and the GHZ case start from zero while the $|W\rangle$ case starts from maximum entanglement $C(\rho_{ab}) = \frac{2}{3}$ and then there is a sudden death [46, 47, 48] and sudden rebirth "anabiosis" [49]. This phenomenon appears in this case as a bipartite subsystem where the third atom and the field are traced.

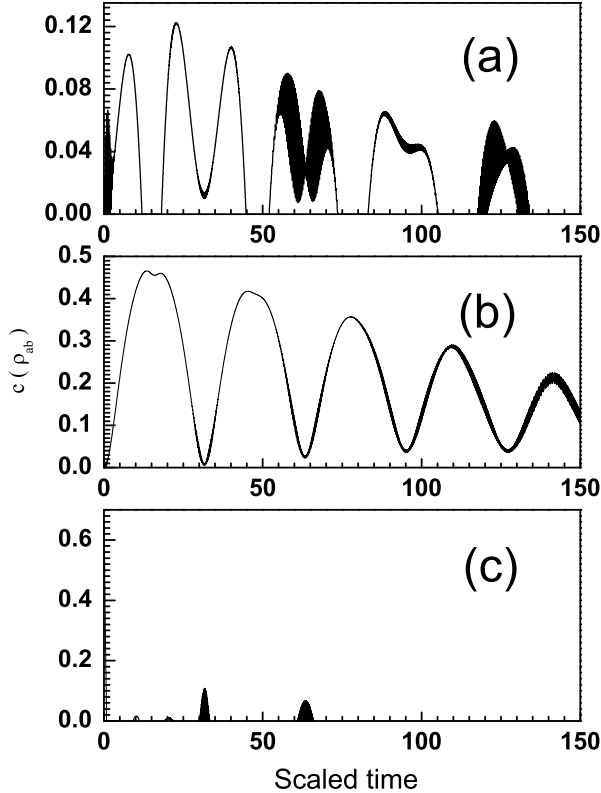


FIG. 3: Evolution of the atoms-pairwise entanglement, by the concurrence of $\hat{\rho}_{ab}$ For (a) $|eee\rangle$ -initial state, (b) $|GHZ\rangle$ -initial state and (c) $|W\rangle$ -initial state.

THREE-PARTICLE RESIDUAL ENTANGLEMENT

By using the notion of negativity [14, 16], we shall study the phenomena of entanglement sharing and the residual 3-particle entanglement "three-way entanglement" [3, 38]. Coffman et al [38] introduced the tangle notation to quantify the entanglement of three qubits A, B, and C in a joint pure state and they discussed entanglement sharing between three particles. They found that unlike classical correlation, quantum entanglement cannot be freely shared among the particles. More precisely they found that the following inequality

$$\tau_{A(BC)} \geq \tau_{AB} + \tau_{AC} \quad (14)$$

holds for any three qubits in a joint pure state. Here the tangle $\tau_{A(BC)}$ is the I-concurrence of Eq.11, between A and the other two qubits as one entity, while the other two tangles τ_{AB} and τ_{AC} are the squares of concurrence Eq.12, between A and B, and A and C respectively. Consequently they defined the 3-tangle (or residual tangle)

τ_{ABC} as follows:

$$\tau_{A(BC)} = \tau_{AB} + \tau_{AC} + \tau_{ABC} \quad (15)$$

To be read, the entanglement of A with the rest of the system is equal to the entanglement of A with B alone, plus the entanglement of A with C alone plus the 3-tangle of the whole system. The 3-tangle quantify the residual three-particle entanglement, which cannot be accounted for by the pairwise entanglement. For the GHZ-state we have $1 = 0 + 0 + \tau_{ABC}$. Also they showed that the inequality (14) is true in case of three particle in a joint mixed state

On the other hand the Peres-Horodecki criterion for separability [12, 13] leads to a natural computable measure of entanglement, called negativity [14, 15, 16]. The negativity is based on the trace norm of the partial transpose ρ^{TA} of the bipartite mixed state ρ_{AB} , and measures the degree to which ρ^{TA} fails to be positive. The density matrices which represent physical systems are non-negative matrices with unit trace, the partial transpose also satisfies $\text{Tr}\{\rho^{TA}\} = 1$, but since it may have negative eigenvalues μ_i for entangled states" therefore its trace norm reads in general

$$\|\rho^{T_1}\|_1 = 1 + 2 \left| \sum_i \mu_i \right| \equiv 1 + \mathcal{N}(\rho) \quad (16)$$

where $\mathcal{N}(\rho)$ is the negativity, i.e. the absolute value of twice the sum of the negative eigenvalues. Vidal and Werner [16] proved that the negativity $\mathcal{N}(\rho)$ is an entanglement monotone and therefore it is a good measure of entanglement. Following [16], the residual three-particle entanglement \mathcal{N}_{abc} in our case can be quantified using the relation

$$\mathcal{N}_{abc} = \mathcal{N}_{a-bc}(\rho_{abc}) - \mathcal{N}_{a-b}(\rho_{ab}) - \mathcal{N}_{a-c}(\rho_{ac}) \quad (17)$$

$$\mathcal{N}_{a-bc}(\rho_{abc}) = \|\rho_{abc}^{T_a}\|_1 - 1 \quad (18)$$

$$\mathcal{N}_{a-b}(\rho_{ab}) = \|\rho_{ab}^{T_a}\|_1 - 1 \equiv \|\rho_{ab}^{T_b}\|_1 - 1 \quad (19)$$

$$\mathcal{N}_{a-c}(\rho_{ac}) = \|\rho_{ac}^{T_a}\|_1 - 1 \equiv \|\rho_{ac}^{T_c}\|_1 - 1 \quad (20)$$

The term $\mathcal{N}_{a-bc}(\rho_{abc})$ quantifies the strength of quantum correlations between the atom "a" and the other two atoms. The remaining two terms quantify the pairwise entanglement between the atom "a" and b or c. Note that the partial trace operation belongs to the set of local operations and classical communication (LOCC) under which the entanglement can not increase. Therefore the left hand side of Eq.17 is a residual three-particle entanglement. In our case $\mathcal{N}_{a-b}(\rho_{ab}) = \mathcal{N}_{a-c}(\rho_{ac})$ because of the symmetry. In Fig.4 we show the results for the different initial states. We see that the residual 3-particle entanglement changes between local maxima and minima during the evolution. The local maxima occur at

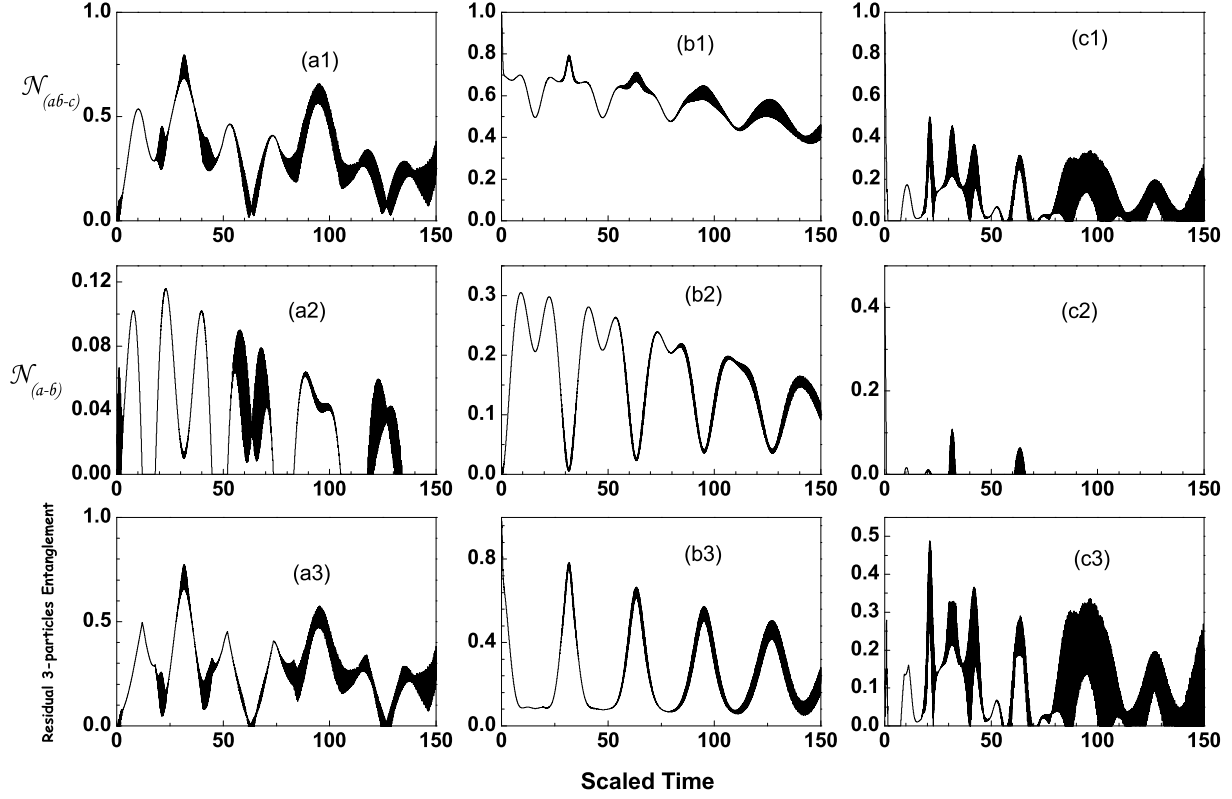


FIG. 4: Evolution of the negativity $\mathcal{N}_{a-bc}(\rho_{abc})$, $\mathcal{N}_{a-b}(\rho_{ab})$ and the residual 3-particles negativity \mathcal{N}_{abc} for different initial atomic states (a) $|eee\rangle$ -initial state, (b) $|GHZ\rangle$ -initial state and (c) $|W\rangle$ -initial state.

half-revival times, when the the atoms became most disentangled from the field. Asymptotically this residual entanglement vanishes and the atomic system becomes maximally entangled with the field. From Figs. 3 and 4 it is shown that the negativity measure of two-atom entanglement is less than or at most equal to the concurrence as it is conjectured in [15].

Q-FUNCTION

In this section we return to the entanglement between the field and the atomic system but through the field dynamic, namely we will discuss the field quasi-probability distribution function, the Q-function [50], defined as $Q(\beta, t) = \frac{1}{\pi} \langle \beta | \rho_f(t) | \beta \rangle$. By using Eq.(5) we get the following form of the Q-function in terms of probability amplitudes.

$$Q(\alpha, t) = \frac{e^{-|\beta|^2}}{\pi} \sum_{i=1}^4 \left| \sum_{n=0}^{\infty} \frac{(\beta^*)^{n+i-1}}{\sqrt{(n+i-1)!}} X_i^{(n)} \right|^2 \quad (21)$$

Figs.5,6, 7 show the Q -function for different initial atomic states at different characteristic times $t_0 = 0$, $t_1 = \frac{\pi}{3}\sqrt{\bar{n}}$, $t_2 = \frac{2\pi}{3}\sqrt{\bar{n}}$, $t_3 = \pi\sqrt{\bar{n}}$, $t_4 = \frac{4\pi}{3}\sqrt{\bar{n}}$, $t_5 = 2\pi\sqrt{\bar{n}}$. The field is initially in a coherent state with average photon number $|\alpha_0|^2 = \bar{n} = 100$. At $\tau = 0$ the shape of the Q -function is a Gaussian centered at $(\sqrt{\bar{n}}, 0)$ as expected for the initial coherent state. But as time develops we found different types of behavior associated with each initial atomic state. For the state $|eee\rangle$ depicted in Fig.5; we note that the single peak is splitted into two pairs, a pair with large amplitude moving slowly in opposite directions and the other pair of the smaller amplitudes moving fastly in opposite directions. To shed some light on this behavior, rough analysis of formula (21), similar to that used in the atomic inversion, shows that time dependent factors in the summand behave like $\{\cos 3(\sqrt{\bar{n}} - \sqrt{\bar{m}})\tau + 3 \cos(\sqrt{\bar{n}} - \sqrt{\bar{m}})\tau\}$. This form exhibits clearly the appearance of the pairs and the first term represents the faster pair while the second term represents the slower pair with amplitude 3 times larger than the faster ones. Note the appearance of the

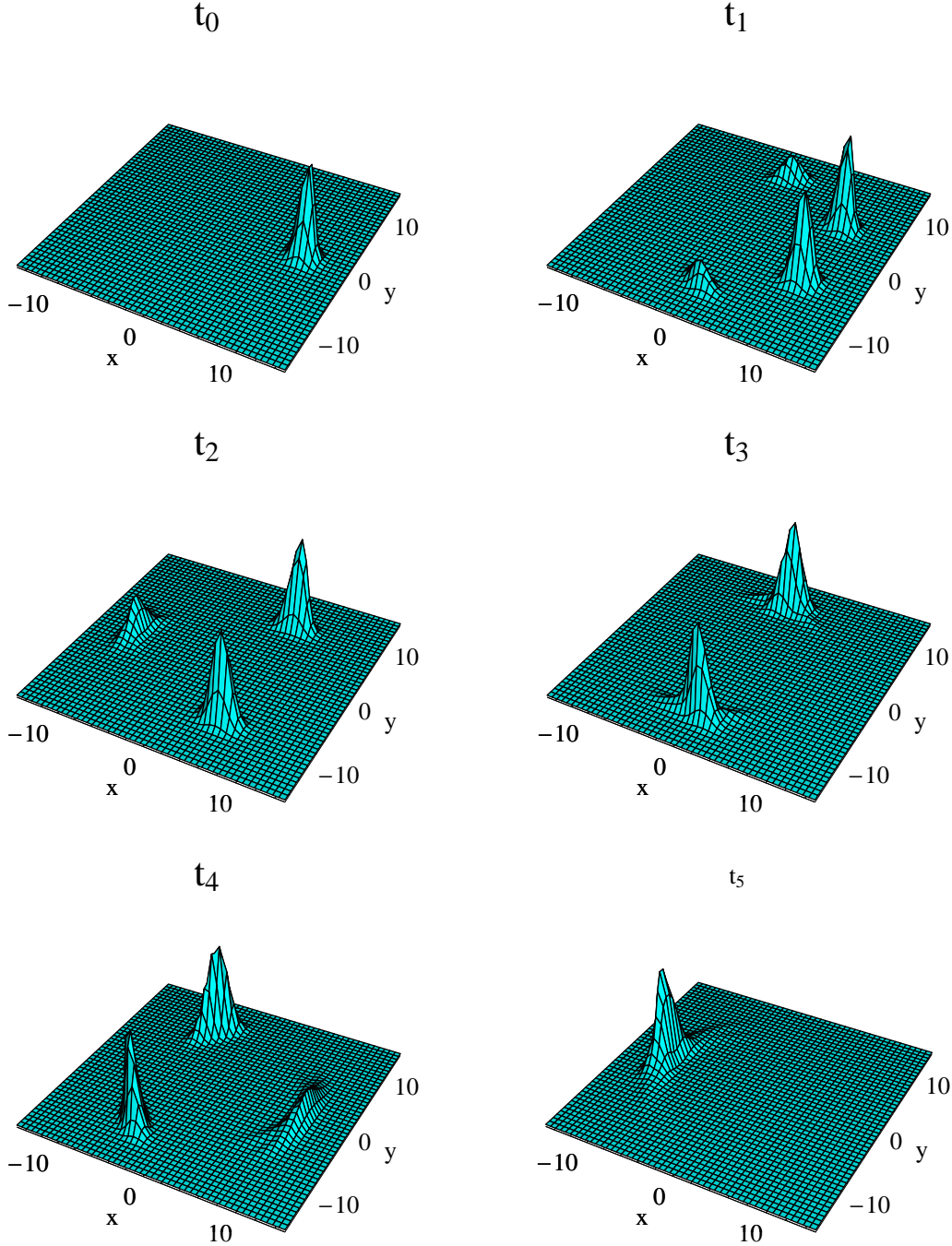


FIG. 5: The Q-function for the initial atomic state $|\Psi(0)\rangle = |eee\rangle$

Schrödinger cat-state [32], at half-revival ($\tau = t_3$). The case of the state $\frac{1}{\sqrt{2}}(|ggg\rangle + |eee\rangle)$ is quite interesting. Here the peak splits into only two peaks; a small faster peak and a large slower peak. The analysis shows that the time-dependent factor in the summand behaves as $\{e^{3i(\sqrt{m}-\sqrt{n})\tau} + 3e^{i(\sqrt{n}-\sqrt{m})\tau}\}$ which exhibits the two single peaks, they move in opposite directions and the

larger is the slower peak. The third case of the Werner state as depicted in Fig.7 shows an opposite behaviour to that of the $|eee\rangle$ state. The pair with the larger amplitude moves faster than the pair with smaller amplitude. The time dependent-factor in the summand in this case behaves like $\{3 \cos 3(\sqrt{n} - \sqrt{m})\tau + \cos(\sqrt{n} - \sqrt{m})\tau\}$ which demonstrates the fast movement of the larger

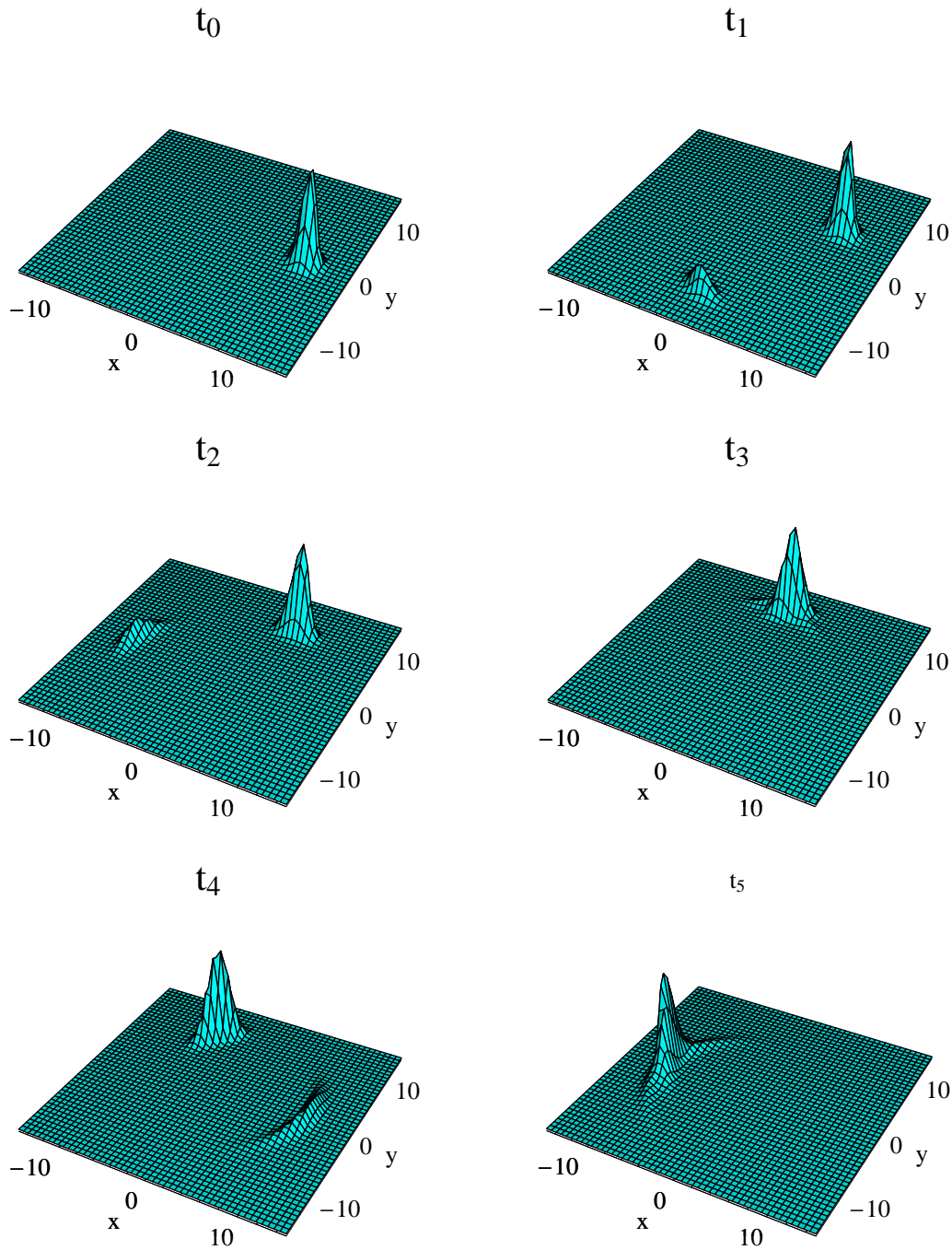


FIG. 6: The Q-function for the initial atomic state $|\Psi(0)\rangle = \frac{1}{\sqrt{2}}(|eee\rangle + |ggg\rangle)$

components and the slow movement of the smaller components. It is to be remarked that at half revival time starting from either the uppermost excited state ($|eee\rangle$) or the Wener state the Schrödinger cat-state is produced. On the other hand starting from the GHZ-state we find that at half revival time the field state returns to its original state. Because as the larger

component moves $\frac{\pi}{2}$ in the phase space the smaller and faster component would move $\frac{3\pi}{2}$ on the other direction and meets the larger one. The previous behavior is also demonstrated in Fig.1.(b) regarding the atomic inversions

Now looking at the various entanglement evolution

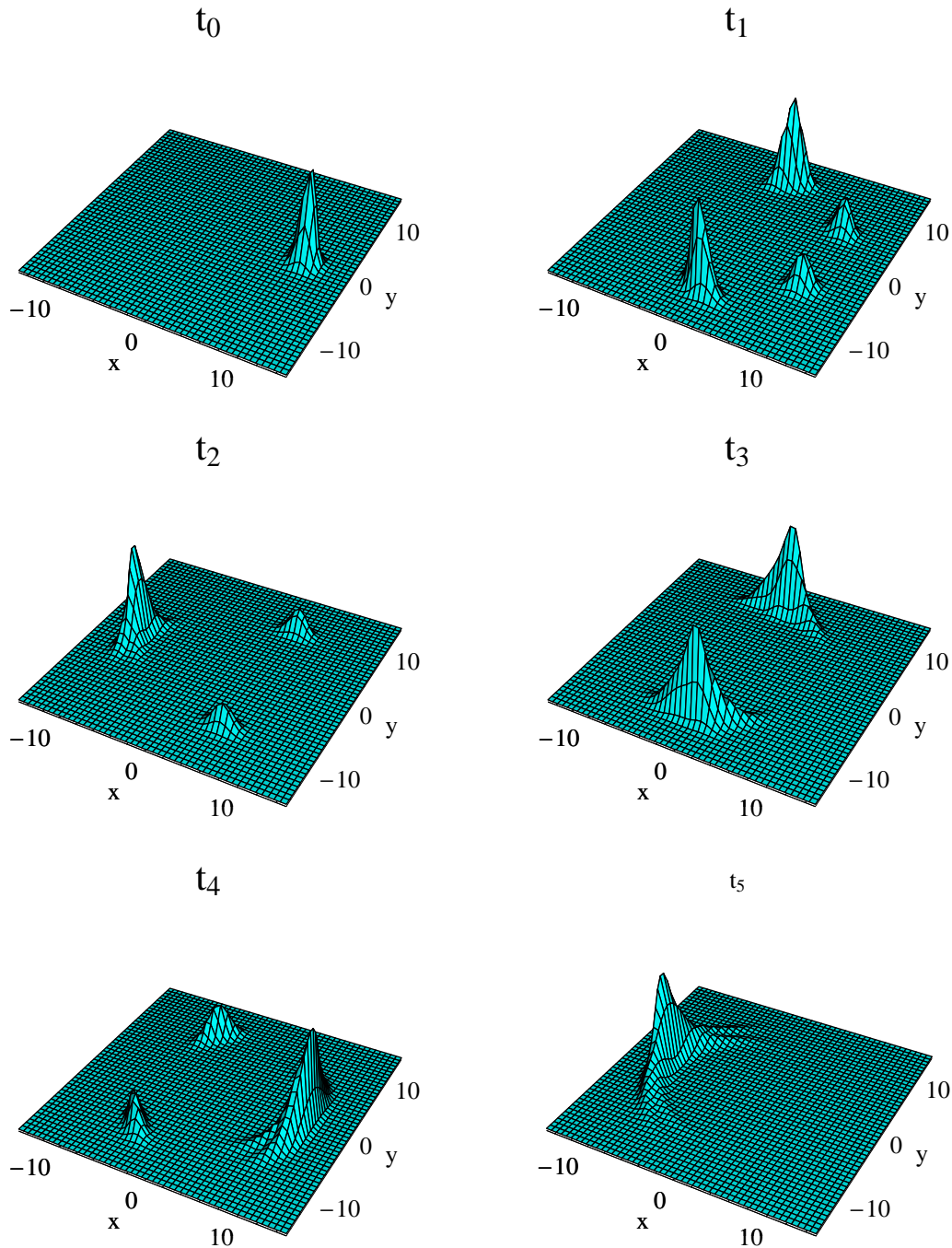


FIG. 7: The Q-function for the initial atomic state $|\Psi(0)\rangle = \frac{1}{\sqrt{3}}(|eeg\rangle + |ege\rangle + |gee\rangle)$

Figs.2 and 4 we find that there is a clear connection between the Q-function dynamic and various entanglement evolutions. For the $|eee\rangle$ and $|W\rangle$ initial states, at half the first-revival time t_1 which correspond to a local minima of I-Concurrence, $I_{f(abc)}$ in the $|eee\rangle$ case and to the minimum value in the $|W\rangle$ case, the faster peaks became most apart from each other. Also at that time the resid-

ual 3-particle entanglement has a local maximum. At the first-revival time t_3 these two peaks collide and recombine, and this corresponds to a local minima of $I_{f(abc)}$ in the two cases, a local minima of the residual 3-particle in $|eee\rangle$ case and a maximum value in the $|W\rangle$ case. Also we note that the amplitude of these two peaks increase significantly in the $|W\rangle$ case. This behavior can be con-

nected to Figs.3.(c1),(c2),(c3), where it is clear that at that time t_4 the entanglement of all the atomic ensembles with the field is minimum and this is not the case in the $|eee\rangle$ state. The last interesting feature we want to mention here for the $|eee\rangle$ and Wener cases is that, at t_5 , the Q-function, shows phase squeezing.

DISCUSSION AND CONCLUSION

In this paper we consider a system of identical three two-level atoms interacting at resonance with a single-mode of the quantized field in a lossless cavity. The initial cavity field is prepared in the coherent state while the atoms are taken in different initial states, namely the atoms taken to be in the excited state, $|eee\rangle$, the GHZ entangled state and the Wener entangled state. For this system we investigated different kinds of entanglement, atoms-field cooperative and atoms-pairwise entanglements. We use the concurrence, the generalized I-concurrence and the negativity as measures of these types of entanglements. The relationship between this entanglement and the collapse and revival in the atomic inversion is investigated. Also the Q -functions for different cases are discussed and connected to different entanglements evolutions of the system. Most noteworthy we found that the GHZ-state is more robust against energy losses, and showing almost coherent trapping. Also one can say that the entanglement of GHZ-state is more robust than the W-state. These two different behav-

iors have been distinctly shown through the study, perfectly depicted in Fig.1.(b1) and Fig.4.(b1) respectively. This suggests that the GHZ-state may show more resistance to the decoherence phenomena than any other three-partite entanglement. Consequently it may be a primary candidate for many quantum information tasks, which need a three-partite entanglement state. In fact the GHZ-state is a resource for many applications, these include, quantum secret sharing [51], open destination teleportation [52] and quantum computation [53]. On the other hand for the other two cases ($|eee\rangle$ and W states) the Schrödinger cat-state is produced. Another interesting feature is the clear link between the Q-function dynamics and various entanglement evolution. Finally we found that, while the W-state, is the state with the maximal possible bipartite entanglement in the reduced two-qubit states, its initial entanglement vanishes very rapidly. Moreover the production of such pairwise entanglement through the evolution is very small. This in contrast to the other two cases which have no pairwise entanglement initially but such entanglement increase greatly through the evolution. Sudden death and sudden revival of atoms-pairwise entanglement are produced with the W-state

APPENDIX : EVOLUTION MATRIX FOR THE PROBABILITIES AMPLITUDES

In this appendix we give the explicit form of the elements of the evolution matrix \mathcal{U} appearing in Eq.(6)

$$\begin{aligned}
\mathcal{U}_{11} &= \left[\frac{\mu_1 - 4\beta^2 - 3\eta^2}{(\mu_1 - \mu_2)} \cos(\sqrt{\mu_1} \tau) + \frac{\mu_2 - 4\beta^2 - 3\eta^2}{(\mu_2 - \mu_1)} \cos(\sqrt{\mu_2} \tau) \right] \\
\mathcal{U}_{12} &= -i\sqrt{3}\gamma \left[\frac{\mu_1 - 3\eta^2}{\sqrt{\mu_1}(\mu_1 - \mu_2)} \sin(\sqrt{\mu_1} \tau) + \frac{\mu_2 - 3\eta^2}{\sqrt{\mu_2}(\mu_2 - \mu_1)} \sin(\sqrt{\mu_2} \tau) \right] \\
\mathcal{U}_{13} &= 2\sqrt{3}\beta\gamma \left[\frac{1}{(\mu_1 - \mu_2)} \cos(\sqrt{\mu_1} \tau) + \frac{1}{(\mu_2 - \mu_1)} \cos(\sqrt{\mu_2} \tau) \right] \\
\mathcal{U}_{14} &= -6i\beta\gamma\eta \left[\frac{1}{\sqrt{\mu_1}(\mu_1 - \mu_2)} \sin(\sqrt{\mu_1} \tau) + \frac{1}{\sqrt{\mu_2}(\mu_2 - \mu_1)} \sin(\sqrt{\mu_2} \tau) \right] \\
\mathcal{U}_{22} &= \left[\frac{\mu_1 - 3\eta^2}{(\mu_1 - \mu_2)} \cos(\sqrt{\mu_1} \tau) + \frac{\mu_2 - 3\eta^2}{(\mu_2 - \mu_1)} \cos(\sqrt{\mu_2} \tau) \right] \\
\mathcal{U}_{23} &= -2i\beta \left[\frac{\sqrt{\mu_1}}{(\mu_1 - \mu_2)} \sin(\sqrt{\mu_1} \tau) + \frac{\sqrt{\mu_2}}{(\mu_2 - \mu_1)} \sin(\sqrt{\mu_2} \tau) \right] \\
\mathcal{U}_{24} &= 2\sqrt{3}\beta\eta \left[\frac{1}{(\mu_1 - \mu_2)} \cos(\sqrt{\mu_1} \tau) + \frac{1}{(\mu_2 - \mu_1)} \cos(\sqrt{\mu_2} \tau) \right] \\
\mathcal{U}_{33} &= \left[\frac{\mu_1 - 3\gamma^2}{(\mu_1 - \mu_2)} \cos(\sqrt{\mu_1} \tau) + \frac{\mu_2 - 3\gamma^2}{(\mu_2 - \mu_1)} \cos(\sqrt{\mu_2} \tau) \right] \\
\mathcal{U}_{34} &= -i\sqrt{3}\eta \left[\frac{\mu_1 - 3\gamma^2}{\sqrt{\mu_1}(\mu_1 - \mu_2)} \sin(\sqrt{\mu_1} \tau) + \frac{\mu_2 - 3\gamma^2}{\sqrt{\mu_2}(\mu_2 - \mu_1)} \sin(\sqrt{\mu_2} \tau) \right] \\
\mathcal{U}_{44} &= \left[\frac{\mu_1 - 4\beta^2 - 3\gamma^2}{(\mu_1 - \mu_2)} \cos(\sqrt{\mu_1} \tau) + \frac{\mu_2 - 4\beta^2 - 3\gamma^2}{(\mu_2 - \mu_1)} \cos(\sqrt{\mu_2} \tau) \right]
\end{aligned}$$

* Electronic address: mohamadmath@yahoo.com

- [1] A. Peres, *Quantum Theory: Concepts and Methods* (Kluwer Academic, Dordrecht, The Netherlands, 1993).
- [2] M. A. Nielsen and I. L. Chuang, *Quantum Computation and Quantum information* (Cambridge University, Cambridge, UK, 2000).
- [3] D. Deutsch, Proc. R. Soc. Lond. A **400**, 97 (1985).
- [4] C. H. Bennet, G. Brassard, C. Crépeau, R. Jozsa, A. Peres, and W. K. Wootters, Phys. Rev. Lett. **70**, 1895 (1993).
- [5] C. H. Bennet and S. Wiesner, Phys. Rev. Lett. **69**, 2881 (1992).
- [6] M. Hillery, V. Bužek, and A. Berthiaume, Phys. Rev. A. **59**, 1829 (1999).
- [7] E. T. Jaynes and F. W. Cummings, Proc. IEEE **51**, 89 (1963).
- [8] B. W. Shore and P. L. Knight, J. Mod. Opt. **40**, 1195 (1993).
- [9] S. J. D. Phoenix and P. L. Knight, Ann. Phys. **186**, 381 (1988).
- [10] J. Gea-Banacloche, Phys. Rev. Lett. **65**, 3385 (1990).
- [11] J. Gea-Banacloche, Phys. Rev. A. **44**, 5913 (1991).
- [12] A. Peres, Phys. Rev. Lett. **77**, 1413 (1996).
- [13] M. Horodecki, P. Horodecki, and R. Horodecki, Phys. Lett. A **223**, 1 (1996).
- [14] K. Zyczkowski, P. Horodecki, A. Sanpera, and M. Lewenstein, Phys. Rev. A **58**, 883 (1998).
- [15] K. Zyczkowski, Phys. Rev. A **60**, 3496 (1999).
- [16] G. Vidal and R. F. Werner, Phys. Rev. A **65**, 032314 (2002).
- [17] R. H. Dicke, Phys. Rev. **93**, 99 (1954).
- [18] M. Tavis and F. W. Cummings, Phys. Rev. **170**, 379 (1968).
- [19] M. Tavis and F. W. Cummings, Ibid. **188**, 692 (1969).
- [20] J. Kempe, Phys. Rev. A **60**, 910 (1999).
- [21] L. Pedersen and C. Rangan, Quantum Information Processing **7**, 33 (2008).
- [22] T. Monz, K. Kim, W. Hänsel, M. Riebe, A. S. Villar, P. Schindler, M. Chwalla, M. Hennrich, and R. Blatt, Phys. Rev. Lett. **102**, 040501 (2006).
- [23] A. Joshi and M. Xiao, Phys. Rev. A **74**, 052318 (2006).
- [24] S. Rai and J. Rai, arXiv:quant-ph/0006107 (2000).
- [25] I. K. Kudryavtsev, A. Lambrecht, H. Moya-Cessa, and P. L. Knight, J. Mod. Opt. **40**, 1605 (1993).
- [26] J. H. Eberly, N. B. Narozhny, and J. J. Sanchez-Mondragon, Phys. Rev. Lett. **44**, 1323 (1980).
- [27] N. B. Narozhny, J. J. Sanchez-Mondragon, and J. H. Eberly, Phys. Rev. A. **23**, 236 (1981).
- [28] H. I. Yoo, J. J. Sanchez-Mondragon, and J. H. Eberly, J. Phys. A. **14**, 1383 (1981).
- [29] H. I. Yoo and J. H. Eberly, Phy. Rep. **118**, 239 (1985).
- [30] S. J. D. Phoenix and P. L. Knight, Phys. Rev. Lett. **66**, 2833 (1991).
- [31] S. J. D. Phoenix and P. L. Knight, Phys. Rev. A. **44**, 6023 (1991).
- [32] V. Bužek, H. Moya-Cessa, P. L. Knight, and S. J. D. Phoenix, Phys. Rev. A. **45**, 8190 (1992).
- [33] W. P. Schleich, *Quantum Optics in Phase Space* (WILEY-VCH, Berlin, 2001).
- [34] W. Vogel and D.-G. Welsch, *Quantum Optics* (WILEY-VCH Verlag Berlin, Berlin, 2006).

- [35] D. M. Greenberger, M. Horne, , and A. Zeilinger, *in Bells Theorem, Quantum Theory, and Conceptions of the Universe* (Kluwer Academic, Dordrecht, The Netherlands, 1989).
- [36] W. Dur, G. Vidal, and J. I. Cirac, *Phys. Rev. A* **62**, 062314/1 (2000).
- [37] K. Zaheer and M. S. Zubairy, *Phys. Rev. A* **39**, 2000 (1989).
- [38] V. Coffman, J. Kundu, and W. K. Wootters, *Phys. Rev. A* **61**, 052306/1 (2000).
- [39] P. Rungta, V. Bužek, C. M. Caves, H. Hillery, and G. J. Milburn, *Phys. Rev. A* **64**, 042315 (2001).
- [40] S. Hill and W. K. Wootters, *Phys. Rev. Lett.* **78**, 5022 (1997).
- [41] R. Alicki and K. Lendi, *Quantum Dynamical Semigroups and Applications* (Springer, Berlin, 1987).
- [42] J. A. S. C. H. Bennett, D. P. DiVincenzo and W. K. Wootters, *Phys. Rev. A* **54**, 3824 (1996).
- [43] C. H. Bennett, H. J. B. S. Popescu, and B. Schumacher, *Phys. Rev. A* **53**, 2046 (1996).
- [44] W. K. Wootters, *Phys. Rev. Lett.* **51**, 2245 (1998).
- [45] T. J. Osborne, *Phys. Rev. A* **72**, 022309 (2005).
- [46] T. Yu and J. Eberly, *Phys. Rev. Lett.* **93**, 140404 (2004).
- [47] Z. Ficek and R. Tanas, *Phys. Rev. A* **74**, 024304 (2006).
- [48] Z. Ficek and R. Tanas, *Phys. Rev. A* **77**, 054301 (2008).
- [49] D. Xiao-Juan and F. Mao-Fa, *Chinese Physics B* **17**, 3209 (2008).
- [50] M. O. Scully and M. S. Zubairy, *Quantum Optics* (University Press, Cambridge, 1997).
- [51] M. Hillery, V. Bužek, and A. Berthiaume, *Phys. Rev. A* **59**, 1829 (1999).
- [52] Z. Zhao, Y.-A. Chen, A.-N. Zhang, T. Yang, H. Briegel, and J.-W. Pan, *Nature* **430**, 54 (2004).
- [53] D. Gottesman and I. Chuang, *Nature* **402**, 390 (1999).

Some Entanglement features of three Atoms Tavis-Cummings Model: Cooperative case

M.Youssef* and A.S.-F.Obada

Department of Mathematics, Faculty of Science, Al-Azhar University, Nasr City, Cairo 11884, Egypt

N.Metwally

Department, Faculty of Science, South Valley University, Aswan, Egypt

(Dated: November 30, 2018)

In this paper we consider a system of identical three two-level atoms interacting at resonance with a single-mode of the quantized field in a lossless cavity. The initial cavity field is prepared in the coherent state while the atoms are taken initially to be either in the uppermost excited state $|eee\rangle$ or The GHZ-state or the W-state. For this system we investigate different kinds of atomic inversion and entanglement, which arise between the different parts of the system due to the interaction. Also the relationship, between entanglement and some other nonclassical effects in the statistical properties, such as collapses and revivals in the atomic inversion where superharmonic effects appear, is discussed. The Q -functions for different cases are discussed. Most remarkably it is found that the GHZ-state is more robust against energy losses, showing almost coherent trapping and Schrödinger-cat states can not be produced from such state. Also the entanglement of GHZ-state is more robust than the W-state. Another interesting feature found is that the state which has no pairwise entanglement initially will have a much improvement of such pairwise entanglement through the evolution. Sudden death and sudden revival of atoms-pairwise entanglement are produced with the W-state.

PACS numbers: 37.30.+i, 03.67.*

INTRODUCTION

The quantum entanglement phenomenon is not only one of the most interesting features of the quantum theory [1], that signifies it from the classical theory, but also lies at the heart of the new rapidly developing area known as the quantum information processing [2]. It is one of the crucial resources required in the applications in this new area of science, which include, quantum computation[3], quantum teleportation [4], quantum dense coding [5] and quantum cryptography [6]. In quantum optics domain, the interaction of an atom with a quantized electromagnetic field mode described by the Jayens-Cumming model[7, 8]leads to an entanglement of these two systems such that the total state vector cannot be written as a product of the time-dependent atomic and field component vectors [9, 10, 11]. To quantify entangled states, one should know whether they are pure or mixed states. Thus, if the entangled state is in a pure state, then it is sufficient to use von Neumann entropy as a measure of entanglement. Many efforts have been devoted to quantify entanglement, particularly for mixed states of a bipartite system, and a number of measures have been proposed, such as entanglement of formation, relative entropy of entanglement and negativity. The Peres-Horodecki criterion for separability [12, 13] leads to a natural computable measure of entanglement, called negativity [14, 15, 16]. It has been proved that the negativity $\mathcal{N}(\rho)$ is an entanglement monotone and therefore can be used as a good measure of entanglement [16].

On the other hand the cooperative nature of the interaction of a quantized radiation field with a system of two-level atoms has first been treated by Dicke [17]. A particular case of the Dicke model, when the atoms interact with a single-mode radiation field inside a cavity was investigated by Tavis and Cummings TCM [18, 19]. The interaction between a field and an ensemble of atoms develop correlations between the field and the atomic systems and between the atomic systems parties as well in the course of their dynamics. Quantifying this quantum correlations(entanglement) is one of the open problems. Multi-qubit systems are of interest to be investigated both theoretically and experimentally. In recent years, great achievements have been made in the application of three-qubit states, because understanding of entanglement and dynamics of three-qubit system is an important matter, for example, it has many applications in quantum cryptography [20], quantum computation [21] and quantum gates [22, 23].

In this paper, we consider a system of identical three two-level atoms interacting at resonance with a single-mode of the quantized field in a lossless cavity. The initial cavity field is prepared in the coherent state while the atoms may assume different initial states. For this system, we investigate some kinds of entanglement which arise between the different parts of the system due to the interaction. We use the concurrence, the generalized I-concurrence and the negativity to quantify entanglement between different parties as well as the

3-particle residual entanglement. Also we look at the relationship between this entanglement and some other nonclassical effects in the statistical properties such as collapses and revivals in the atomic inversion. The field dynamics and atoms-field entanglement are discussed through Q -function.

This paper is organized as follows. In section 2 we introduce the system and its solution. Section 3 is devoted to the atomic inversions. In section 4 we study the field atom entanglement, two-atom entangle and the atomic system purity. Section 5 is devoted to the residual 3-particle entanglement. The field dynamics in phase space, the possibility of having a cat state and the atoms-field entanglement are addressed in section 6. Finally in section 7. we conclude the paper with a discussion of the results.

THE MODEL AND ITS TIME EVOLUTION

We consider a system of three identical two-level atoms interacting with a quantized single-mode electromagnetic field. Under the rotating-wave approximation and resonant condition, the Hamiltonian of this system reads:

$$\begin{aligned} \hat{H} = \hat{H}_0 + \hat{H}_I = \omega_f \left(\hat{a}^\dagger \hat{a} + \frac{1}{2} \sum_{i=a,b,c} \hat{\sigma}_z^{(i)} \right) \\ + g \left(\hat{a} \sum_{i=a,b,c} \hat{\sigma}_+^{(i)} + \hat{a}^\dagger \sum_{i=a,b,c} \hat{\sigma}_-^{(i)} \right) \end{aligned} \quad (1)$$

where ($\hbar = 1$). The terms \hat{H}_0 and \hat{H}_I represent the free and interaction hamiltonians respectively; ω_f is the field frequency, and equals the atomic transition frequency on resonance; $\hat{\sigma}_+^{(i)}$, $\hat{\sigma}_-^{(i)}$ and $\hat{\sigma}_z^{(i)}$ are the the usual raising, lowering and inversion operators for the i^{th} atom, satisfying $[\hat{\sigma}_+^{(i)}, \hat{\sigma}_-^{(i)}] = \hat{\sigma}_z^{(i)}$, $[\hat{\sigma}_z^{(i)}, \hat{\sigma}_\pm^{(i)}] = \pm 2\hat{\sigma}_\pm^{(i)}$, $[\hat{\sigma}_\mu^{(i)}, \hat{\sigma}_\nu^{(j)}] = 0$ while $\hat{a}^\dagger(\hat{a})$ is the Bose creation (annihilation) operator for the quantized field mode satisfying the commutation relations $[\hat{a}, \hat{a}^\dagger] = 1$, and g is the coupling constant. Since $[\hat{H}_0, \hat{H}_I] = 0$, it follows that, the Hamiltonian (1) conserves the total number of excitations N , i.e. the total excitation operator

$$\hat{N} = \hat{a}^\dagger \hat{a} + \frac{1}{2} \sum_{i=a,b,c} \hat{\sigma}_z^{(i)} \quad (2)$$

is a constant of motion. This provides a decomposition for the system Hilbert space as $\mathcal{H} = \sum_{n=0}^{\infty} \oplus \mathcal{H}_n$ such that, $\mathcal{H}_0 = \{|g, g, g; 0\rangle\}$, $\mathcal{H}_1 = \{|g, g, g; 1\rangle, |g, e, g; 0\rangle, |g, g, e; 0\rangle, |e, g, g; 0\rangle\}$ and $\mathcal{H}_2 = \{|g, g, g; 2\rangle, |e, g, g; 1\rangle, |g, e, g; 1\rangle, |g, g, e; 1\rangle, |e, e, g; 0\rangle, |e, g, e; 0\rangle, |g, e, e; 0\rangle\}$ are a one-dimensional, 4-dimensional and 7-dimensional eigensubspaces of N and

$\mathcal{H}_{n+3}|_{n=0}^{\infty} = \{|eee; n\rangle, |eeg; n+1\rangle, |ege; n+1\rangle, |gee; n+1\rangle, |egg; n+2\rangle, |geg; n+2\rangle, |gge; n+2\rangle, |ggg; n+3\rangle\}$

are the eight-dimensional eigensubspaces of N . In the Hilbert space constituted by the above basis, the interaction \hat{H}_I is a diagonal blocks matrix made up of 8×8 sub-matrices, every sub-matrix represents a subspace corresponding to a definite excitation number N . However we found that it is more appropriate for this system to use the Dicke states [17] as a basis, because of the degeneracy produced by the symmetry. For N spin-1/2 particle system, the Dicke states are defined as the states $|S, m_s\rangle$ that are common eigenstates of both the square of the total spin operator \hat{S}^2 and its component along z -axis "the quantization axis" \hat{S}_z with the corresponding eigenvalues $S(S+1)\hbar$ and $m_s\hbar$. For our system the Dicke states in terms of the above mentioned product states are given by

$$\begin{aligned} |\mathcal{D}_1\rangle &= |eee; n\rangle \\ |\mathcal{D}_2\rangle &= \frac{1}{\sqrt{3}} (|eeg; n+1\rangle + |ege; n+1\rangle + |gee; n+1\rangle) \\ |\mathcal{D}_3\rangle &= \frac{1}{\sqrt{3}} (|egg; n+2\rangle + |geg; n+2\rangle + |gge; n+2\rangle) \\ |\mathcal{D}_4\rangle &= |ggg; n+3\rangle \\ |\mathcal{D}_5\rangle &= \frac{1}{\sqrt{6}} (2|gee; n+1\rangle - |ege; n+1\rangle - |eeg; n+1\rangle) \\ |\mathcal{D}_6\rangle &= \frac{1}{\sqrt{2}} (|eeg; n+1\rangle - |ege; n+1\rangle) \\ |\mathcal{D}_7\rangle &= \frac{1}{\sqrt{6}} (|geg; n+2\rangle + |gge; n+2\rangle - 2|egg; n+2\rangle) \\ |\mathcal{D}_8\rangle &= \frac{1}{\sqrt{2}} (|gge; n+2\rangle - |geg; n+2\rangle) \end{aligned} \quad (3)$$

The first four states are fully symmetric with respect to the permutation of particles, while the other four states are in fact a two state of mixed symmetry, which correspond to two degenerate representations, each of dimension 2 [24]. By substituting into the Schrödinger equation $-i \frac{d|\Psi(\tau)\rangle}{d\tau} = \hat{H}_I |\Psi(\tau)\rangle$, where $\tau = gt$, then the wave function generally can be written as $|\Psi(\tau)\rangle = \sum_{i=1}^8 X_i^{(n)}(\tau) |\mathcal{D}_i\rangle$.

We found, as expected, that the equations of the probability amplitudes which correspond to the two degenerate states are decoupled from each other and from the four amplitudes which correspond to the fully symmetric Dicke states. The initial state of the system will be taken as follows:

$$\begin{aligned} |\Psi(0)\rangle &= |\Psi_a(0)\rangle \otimes |\Psi_f(0)\rangle \\ |\Psi_a(0)\rangle &= C_e |e, e, e\rangle + \frac{1}{\sqrt{3}} C_{w1} (|e, e, g\rangle + |e, g, e\rangle + |g, e, e\rangle) \\ &\quad + \frac{1}{\sqrt{3}} C_{w2} (|g, g, e\rangle + |g, e, g\rangle + |e, g, g\rangle) + C_g |g, g, g\rangle \\ |\Psi_f(0)\rangle &= \sum_{n=0}^{\infty} q_n |n\rangle; \quad q_n = e^{(-|\alpha_0|^2/2)} \frac{\alpha_0^n}{\sqrt{n!}} \end{aligned} \quad (4)$$

where $|C_e|^2 + |C_{w1}|^2 + |C_{w2}|^2 + |C_g|^2 = 1$. For the above initial atomic states the wave function evolve only inside the subspace spanned by the fully symmetric Dicke states and the probability amplitudes of the other state vanishes, hence our system is equivalent to a four-level Dicke atom. This is a generalization to the case of two identical atoms [25], where the antisymmetric states do not participate in the dynamics. Solving the coupled four equations of the probability amplitudes we get the wave function of system at any time

$$\begin{aligned} |\Psi(\tau)\rangle &= \sum_{n=0}^{\infty} \sum_{i=1}^4 X_i^{(n)}(\tau) |\mathcal{D}_i\rangle \\ X(\tau) &= [X_1^{(n)}(\tau), X_2^{(n)}(\tau), X_3^{(n)}(\tau), X_4^{(n)}(\tau)]^T \\ &= \mathcal{U}X(0) \end{aligned} \quad (5)$$

where the evolution matrix \mathcal{U} is given by

$$\mathcal{U} = \begin{pmatrix} \mathcal{U}_{11} & \mathcal{U}_{12} & \mathcal{U}_{13} & \mathcal{U}_{14} \\ \mathcal{U}_{21} & \mathcal{U}_{22} & \mathcal{U}_{23} & \mathcal{U}_{24} \\ \mathcal{U}_{31} & \mathcal{U}_{32} & \mathcal{U}_{33} & \mathcal{U}_{34} \\ \mathcal{U}_{41} & \mathcal{U}_{42} & \mathcal{U}_{43} & \mathcal{U}_{44} \end{pmatrix} \quad (6)$$

The explicit form of the matrix elements are given in the appendix, where in there we have

$$\begin{aligned} \mu_{1,2} &= \frac{1}{2} \left(\delta \pm \sqrt{\delta^2 - 36\eta^2\gamma^2} \right) \\ \delta &= (4\beta^2 + 3\gamma^2 + 3\eta^2) \\ \gamma &= \sqrt{n+1}, \quad \beta = \sqrt{n+2}, \quad \eta = \sqrt{n+3} \end{aligned} \quad (7)$$

Note that $X_i^{(n)}$ has q_{n+i-1} as a factor, where $i=1,2,3,4$. By using this wave function, we discuss different aspects of the system in what follows.

ATOMIC INVERSIONS

Energy is the primary quantity determining the properties of physical systems. The atomic inversion and levels occupation probabilities are the simplest nontrivial physical quantities in the atom-field interaction, that display the exchange of energy between the field and the atoms. More important to our investigation, the atomic inversions display the primary nonclassical effect namely, the collapse and revival structure [26, 27, 28, 29] from which we can have information about the atoms-field entanglement and disentanglement through the dynamics [9, 10, 11, 30, 31, 32]. Finally the collapses and revivals will be clearly connected to the evolution of the Q-function [33, 34]. In this section we shall discuss these quantities. We shall deal with three quantities namely,

$$W_T(t) = \sum_{n=0}^{\infty} \left\{ |X_1^{(n)}|^2 - |X_4^{(n)}|^2 \right\} \quad (8)$$

$$\begin{aligned} W_a(t) &= \langle \Psi(t) | \hat{\sigma}_z^{(a)} | \Psi(t) \rangle = \sum_{n=0}^{\infty} \left\{ |X_1^{(n)}|^2 + \frac{1}{3} |X_2^{(n)}|^2 \right. \\ &\quad \left. - |X_4^{(n)}|^2 - \frac{1}{3} |X_3^{(n)}|^2 \right\} \end{aligned} \quad (9)$$

$$P_{ini}(t) = |\langle \Psi(0) | \Psi(t) \rangle|^2 \quad (10)$$

where, $W_T(t)$ is the total atomic inversion, $W_a(t)$ is the inversion of the atom a and $P_{ini}(t)$ is the probability of occupation of the initial state. The two-atoms inversion is double the one-atom inversion. In Fig.1 we show these quantities for the atoms being initially (a) in the excited state $|\Psi_a(0)\rangle = |eee\rangle$, or (b) the atoms initially in a GHZ-state [35], $|\Psi_a(0)\rangle = |\text{GHZ}\rangle = \frac{1}{\sqrt{2}}(|ggg\rangle + |eee\rangle)$, which has the property that tracing over any one qubit results in a maximally mixed state containing no entanglement between the remaining two qubits or (c) in genuine entangled W-state "Werner state" [36], $|\Psi_a(0)\rangle = |W\rangle = \frac{1}{\sqrt{3}}(|eeg\rangle + |ege\rangle + |gee\rangle)$, for this state when tracing over any one qubit the average remaining bipartite entanglement is maximal. Before we dwell in the discussion of the figures we present a rough analysis about the time dependent quantities in the expressions (8, 9 and 10). Since we are dealing with a coherent state for which $\bar{n} = 100$, it is well known that the effective excitation will be due to the photons within the range $|n - \bar{n}| \leq \Delta n = \sqrt{\bar{n}}$. For these photons and those within a reasonably range to them, the radicands appearing in the expressions for β , γ and η in Eq.(7) can be approximated to $\sqrt{\bar{n}}$ and the expressions for μ_1 , μ_2 are then given by "9n" and "n" respectively. Thus the Rabi frequencies appearing in the expressions for \mathcal{U}_{ij} are to be approximated as $3\sqrt{\bar{n}}$ and $\sqrt{\bar{n}}$ respectively. Keeping these points in mind, we find the following for the case of the atomic initial state $|\Psi_a(0)\rangle = |eee\rangle$, i.e., the three atoms are in their excited states: Regarding the quantity $W_T(\tau)$, the time-dependent summand is proportional to $\frac{1}{16}(\cos 6\sqrt{\bar{n}}\tau + 15 \cos 2\sqrt{\bar{n}}\tau)$, containing superharmonics which results in three revival times $\frac{2\pi}{3}\sqrt{\bar{n}}$, $\frac{4\pi}{3}\sqrt{\bar{n}}$ and $2\pi\sqrt{\bar{n}}$ related to the trigonometric functions with two equal heights for the 1st and 2nd revival and 16 times larger at the 3rd revival. This appears clearly in Fig.1.(a1). On the other hand for the single atom population inversion $W_a(t)$, the time dependent summand is proportional to $\cos 2\sqrt{\bar{n}}\tau$, which results in a single revival time at $2\pi\sqrt{\bar{n}}$ which is depicted in Fig.1.(a2). The $P_{ini}(\tau)$ has the term $\frac{1}{32}(10 + \cos 6\sqrt{\bar{n}}\tau + 6 \cos 4\sqrt{\bar{n}}\tau + 15 \cos 2\sqrt{\bar{n}}\tau)$ in its summand, composed of 2 and 3 superharmonics giving rise to revivals times at $\frac{2\pi}{3}\sqrt{\bar{n}}$, $\pi\sqrt{\bar{n}}$, $\frac{4\pi}{3}\sqrt{\bar{n}}$ and $2\pi\sqrt{\bar{n}}$. The second revival is larger than the 1st and 3rd because of the coefficients of $\cos 6\sqrt{\bar{n}}\tau$ and $\cos 4\sqrt{\bar{n}}\tau$ whiles the 4th, at $2\pi\sqrt{\bar{n}}$, is the highest as the four revivals coincide. This is shown faithfully in Fig.1.(a3) whereas the quantity P_{ini} fluctuates around $\frac{5}{16}$.

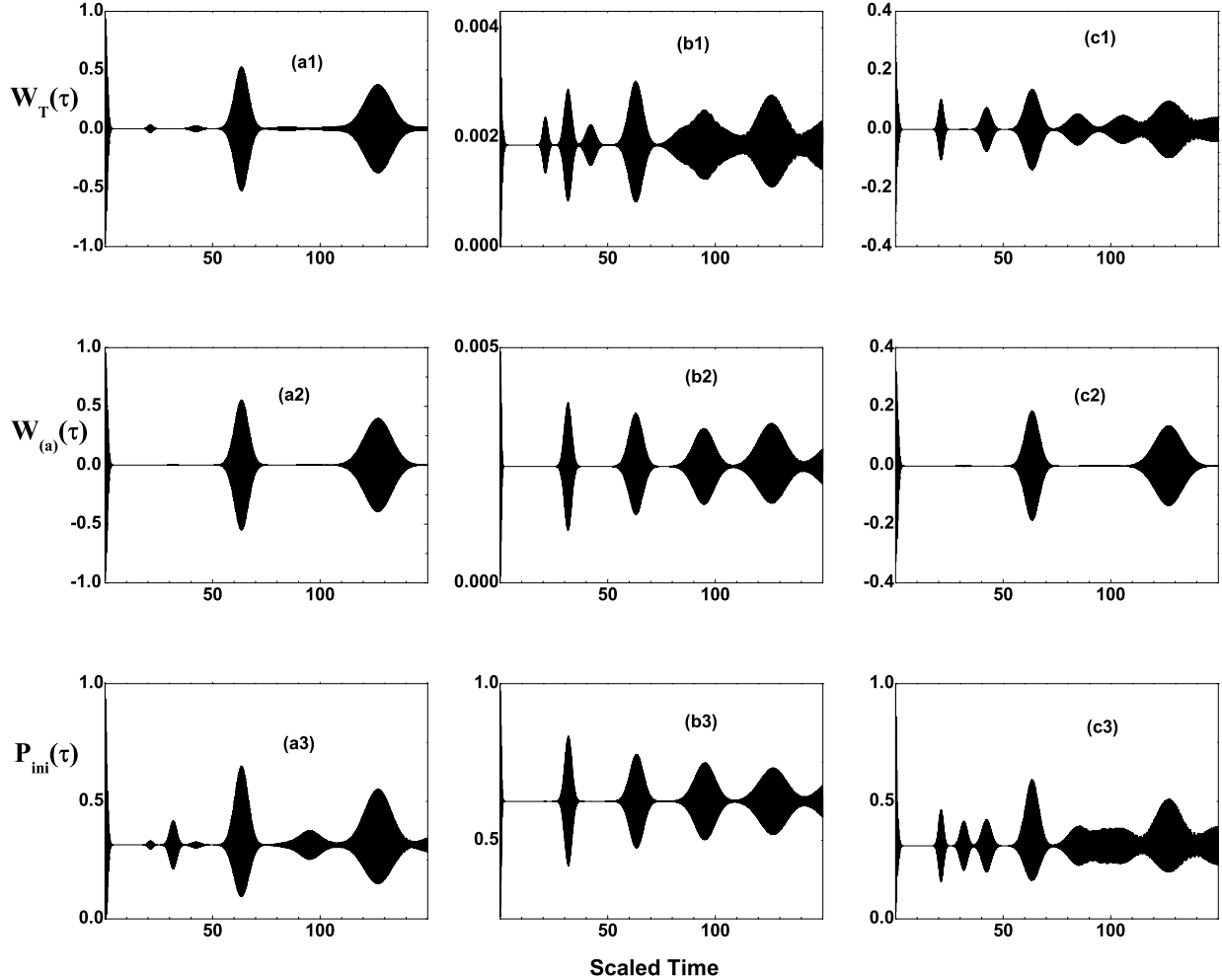


FIG. 1: Evolution of the total atomic inversions $W_T(\tau)$, single-atom inversions $W_a(\tau)$ and the initial state populations $P_{ini}(\tau)$, Eq.(??) for different initial atomic states (a) $|eee\rangle$ -initial state, (b) $|GHZ\rangle$ -initial state and (c) $|W\rangle$ -initial state. The field in a coherent state with $|\alpha|^2 = 100$

Now we look at the initial state $|\Psi_a(0)\rangle = \frac{1}{\sqrt{2}}(|ggg\rangle + |eee\rangle)$ Figs.1(1b,2b,3b), and applying the same analysis as in the previous case, we find the following:- The quantity $W_T(\tau)$ as well as $W_a(\tau)$ is almost zero as can be seen from Fig.1(b1) and Fig.1(b2). In contrast, the quantity $P_{ini}(\tau)$ depends on the summand of the form $\frac{1}{8}(5 + \cos 4\sqrt{n}\tau)$ which results in revival times $\pi\sqrt{n}$ and $2\pi\sqrt{n}$ shown clearly in Fig.1(b3). Also it exhibits the fluctuations around $\frac{5}{8}$. These results show that, starting from the GHZ-state would result in coherent trapping and the atoms almost do not interact with the field. This is shown in the value of $\frac{5}{8}$ for the probability for the atoms staying in the initial state.

The case of the atomic initial Werner state namely

$|\Psi_a(0)\rangle = \frac{1}{\sqrt{3}}(|eeg\rangle + |ege\rangle + |gee\rangle)$ is shown in Figs.1(c1,c2,c3). Analysis of the summand of $W_T(\tau)$ reveals that the time-dependence is of the form $(\cos 6\sqrt{n}\tau + \cos 2\sqrt{n}\tau)$. This amounts to the revival times $\frac{2\pi}{3}\sqrt{n}$, $\frac{4\pi}{3}\sqrt{n}$ and $2\pi\sqrt{n}$ with the amplitude at the 3rd revival twice as much as the 1st revival. Whereas the single atom population inversion has a single revival at $2\pi\sqrt{n}$ because the time dependent term in the summand is proportional to $\cos 2\sqrt{n}\tau$. It is worthnoting that the fluctuations in the population inversion are the highest for the $|eee\rangle$ initial state and the lowest for the GHZ initial state showing an almost coherent trapping [37] for the latter in such a way to resist exchange of energy with the field, whereas the W-state is in the middle, showing a modest degree of exchange of the energy with the field.

COOPERATIVE AND ATOMS-PAIRWISE ENTANGLEMENT

The system under investigation is a multipartite system initially in an over all pure state, occupying the following Hilbert space $\mathcal{H} = \mathcal{H}_a \otimes \mathcal{H}_b \otimes \mathcal{H}_c \otimes \mathcal{H}_f$ with dimension $2 \otimes 2 \otimes 2 \otimes \infty$. Since we consider here only the cooperative case, whereas the Hamiltonian is symmetric under atom exchange, thus there are only eight nonequivalent partitions of bipartite subsystems namely: (i) $f \otimes (abc)$, $(fc) \otimes ab$, $(fcb) \otimes a$, (ii) $f \otimes (ab)$, (iii) $f \otimes a$, (iv) $(fb) \otimes a$, (v) $a \otimes (bc)$ and (vi) $a \otimes b$, corresponding to the field times the whole atomic system, two-atoms times the field with the remaining atom, one-atom times the field with the other two atoms, the field times two-atoms, the field times one-atom, one atom times the field with one-atom, one-atom times the other two atoms and one-atom times one-atom respectively.

These partitions except (i), are obtained by tracing over one or more Hilbert-subspaces of the total Hilbert space and hence they are generally mixed states. For convenience and simplicity we will only study the entanglement evolution of the partitions (i) and the entanglement of the last partition, i.e. atom-atom entanglement. In the following section the entanglement of the bipartite partition (v), will be discussed together with the phenomenon of entanglement sharing [3, 38] and the residual 3-particle entanglement using the negativity.

For the bipartite partitions in (i), each one of them start from an over all pure state and a number of widely accepted measures of entanglement are available. An easier way to quantify the entanglement in this bipartite partitions is to use the square of the pure-state I-concurrence introduced in Ref. [39],

$$C^2(\Psi) = 2\nu_{d_1}\nu_{d_2}[1 - \text{Tr}\{\rho_f^2\}] = 2\nu_{d_1}\nu_{d_2}[1 - \text{Tr}\{\rho_{abc}^2\}] \quad (11)$$

This generalizes the original concurrence's notion introduced by Hill and Wootters [40] $C(\Psi) \equiv \sqrt{\langle \Psi | S_2 \otimes S_2 | \Psi \rangle \langle \Psi | \Psi \rangle} = |\langle \Psi | \sigma_y \otimes \sigma_y | \Psi^* \rangle|$ for pairs of qubits in a joint pure state $|\Psi\rangle$, to be applied for pairs of quantum systems of arbitrary dimension $d_1 \otimes d_2$ in a joint pure state. The concurrence is defined with the help of a superoperator S_2 , whose action on a qubit density operator $\rho = |\Psi\rangle\langle\Psi|$ is to flip the spin of the qubit density operator $S_2(\rho) = \rho^*$; $\rho^* = |\tilde{\Psi}\rangle\langle\tilde{\Psi}|$, where $|\tilde{\Psi}\rangle = \sigma_y \otimes \sigma_y |\Psi^*\rangle$, the asterisk denotes the complex conjugate and σ_y is the Pauli matrix. Rungta et al. [39] use the formalism for superoperators [41] to generalize the spin-flip superoperator S_2 for a qubit to a superoperator S_d that acts on qudit states (d-dimensional states). For defining an I-concurrence, one should choose the scaling factor ν_d to be independent of d , otherwise, the pure state I-concurrence could be

changed simply by adding extra, unused dimensions to one of the subsystems. To be consistent with the qubit concurrence, one should choose $\nu_d = 1$. With this choice the pure-state I-concurrence runs from zero for product states to $I_{max} = \sqrt{\frac{2(m-1)}{m}}$, where $m = \min(d_1, d_2)$, for a maximally entangled state. Henceforth we will use only the term I-concurrence when refereing to it.

On the other hand, Wootters extended the concurrence notation to the case of a two qubits in an arbitrary joint mixed state, he showed that the entanglement of formation [42, 43] of an arbitrary two-qubits mixed state ρ can be written in terms of the minimum average pure-state concurrence of ensemble decompositions of ρ , and he derived an explicit expression for this minimum in terms of the eigenvalues of $\rho\tilde{\rho}$ [44].

$$C(\rho) = \max\{0, \lambda_1 - \lambda_2 - \lambda_3 - \lambda_4\} \quad (12)$$

where λ_i 's are the eigenvalues, in decreasing order, of the Hermitian matrix $R = \sqrt{\sqrt{\rho}\tilde{\rho}\sqrt{\rho}}$. Alternatively, one can say that the λ_i 's are the square roots of the eigenvalues of the matrix $\rho\tilde{\rho}$ and each λ_i is a non-negative real number. The spin-flipped state $\tilde{\rho}$ is obtained by spin flipping, namely $\tilde{\rho} = (\sigma_y \otimes \sigma_y)\rho^*(\sigma_y \otimes \sigma_y)$. where again the asterisk denote the complex conjugate. For a pure state $|\Psi\rangle$, R has only one eigenvalue that may be nonzero, namely, $C(\Psi)$ Eq.(11). Wootters called this minimum average, the concurrence of the mixed state. The entanglement of the last partition, i.e. atom-atom entanglement can be investigated using this formula.

It is worthnoting that the remanning partitions are all in a mixed state with dimensions $2 \otimes \infty$, $4 \otimes \infty$ and $2 \otimes 4$, which can not be quantified by any of the above mentioned entanglement measures. Following Tessier et al. [3], we can quantify the entanglement for all the above partitions using Osborne's formula [45] for the I-tangle $\tau(\rho_{AB})$ for mixed states ρ_{AB} of a pair AB of qudits, of dimensions d_A and d_B , having no more than two nonzero eigenvalues, i.e., ρ_{AB} with rank no greater than 2. The I-tangle τ between A and B is given by the expression

$$\tau(\rho_{AB}) = \text{Tr}\{\rho_{AB}\tilde{\rho}_{AB}\} + 2\lambda_{min}(1 - \text{Tr}\{\rho_{AB}^2\}) \quad (13)$$

where λ_{min} is is the smallest eigenvalue of the real symmetric 3×3 matrix M as defined in [45]

In Fig.2 we show the I-concurrence of the reduced density matrices ρ_{abc} , ρ_{ab} and ρ_a , (a) for the $|eee\rangle$ case, (b) the $|GHZ\rangle$ case and (c) the $|W\rangle$ case. This type of entanglement may be called a cooperative entanglement. Figs.2(a1,a2,a3,b1,c1) begin from zero which corresponds to the initial product state while Figs.(b2,b3,c2,c3) start from 3-particle maximum entanglement state. They suddenly increase in the collapse region to reach the maximum values, $I_{max} = 1.34, 1.23$ and 1 for $f \otimes (abc)$,

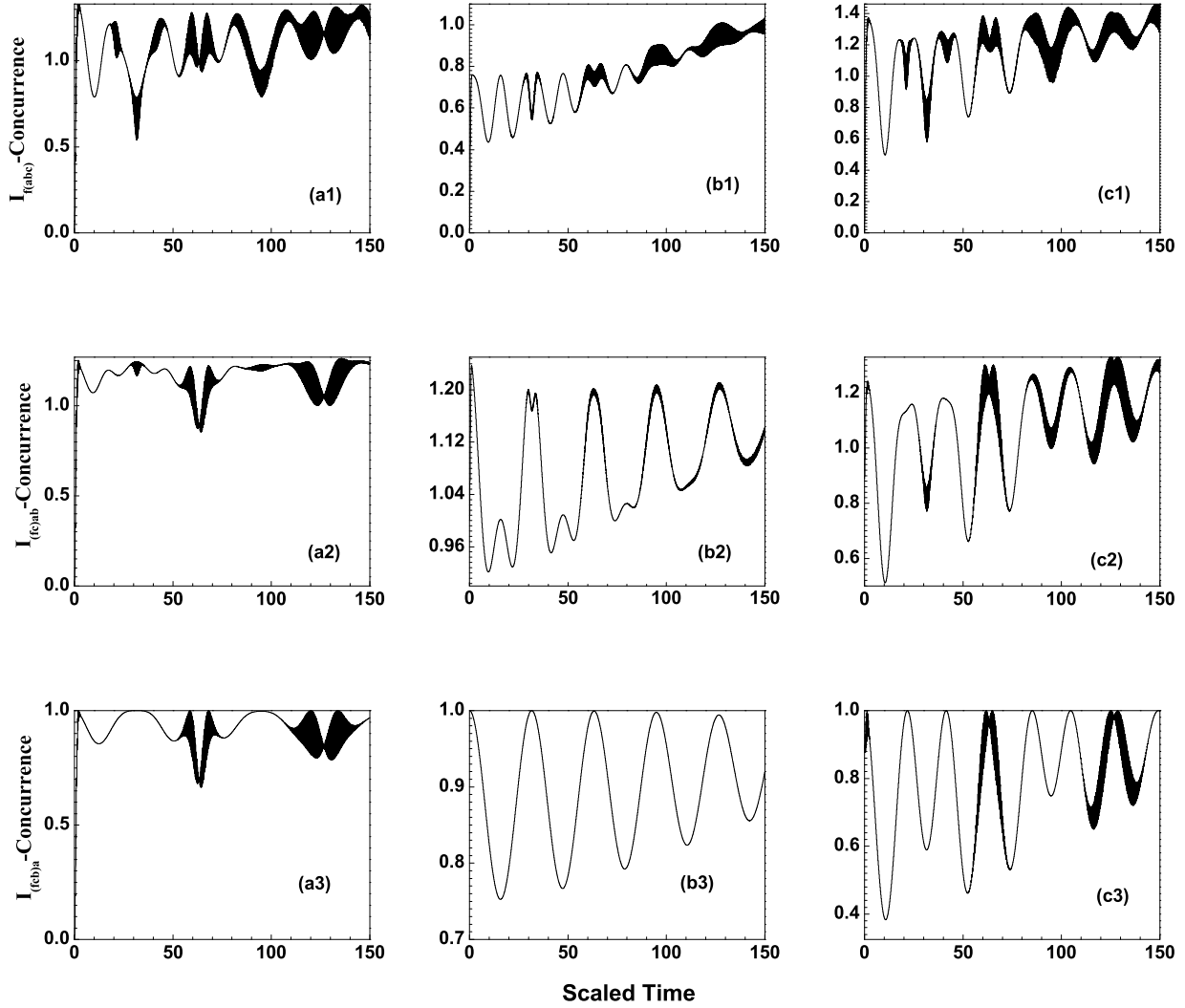


FIG. 2: The I-concurrence for the three bipartite partitions in (i), (a) $|eee\rangle$ -initial state, (b) $|GHZ\rangle$ -initial state and (c) $|W\rangle$ -initial state.

$(fc) \otimes ab$ and $(cb) \otimes a$ respectively. The exception is the entanglement between the field and the total atomic system in the case of the GHZ-state in Fig.2(b1), which did not reach this maximum. This reflects the robustness of the initial entanglement of this state, i.e., the initial entanglement between the atoms resists the interaction and the energy exchange between them and the field as shown in the discussion of the population inversion of last section. When this entanglement becomes rather weak the field-atoms entanglement increase rapidly to the maximum value I_{max} . On the other hand the W-state case did not show such robustness. There are many local minima and maxima asymptotically increasing to reach the maximum values, I_{max} . It is noticed that the GHZ-state

shows more periodicity than the other two cases. Finally, it is clear that the local maxima and minima of the $f \otimes (abc)$ and $(a) \otimes fbc$ figures are opposite to each other. Fig.3 shows the concurrence of the reduced density matrix $C(\rho_{ab})$ for the different initial states. In contrast to the above cooperative entanglement, the atom-atom entanglement asymptotically decreases and vanishes. The initially excited atoms and the GHZ case start from zero while the $|W\rangle$ case starts from maximum entanglement $C(\rho_{ab}) = \frac{2}{3}$ and then there is a sudden death [46, 47, 48] and sudden rebirth "anabiosis" [49]. This phenomenon appears in this case as a bipartite subsystem where the third atom and the field are traced.

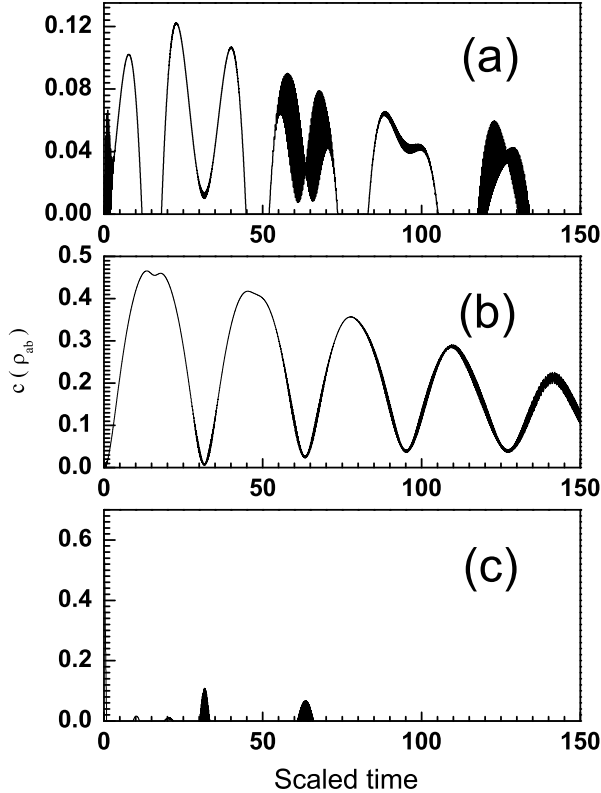


FIG. 3: Evolution of the atoms-pairwise entanglement, by the concurrence of $\hat{\rho}_{ab}$ For (a) $|eee\rangle$ -initial state, (b) $|GHZ\rangle$ -initial state and (c) $|W\rangle$ -initial state.

THREE-PARTICLE RESIDUAL ENTANGLEMENT

By using the notion of negativity [14, 16], we shall study the phenomena of entanglement sharing and the residual 3-particle entanglement "three-way entanglement" [3, 38]. Coffman et al [38] introduced the tangle notation to quantify the entanglement of three qubits A, B, and C in a joint pure state and they discussed entanglement sharing between three particles. They found that unlike classical correlation, quantum entanglement cannot be freely shared among the particles. More precisely they found that the following inequality

$$\tau_{A(BC)} \geq \tau_{AB} + \tau_{AC} \quad (14)$$

holds for any three qubits in a joint pure state. Here the tangle $\tau_{A(BC)}$ is the I-concurrence of Eq.11, between A and the other two qubits as one entity, while the other two tangles τ_{AB} and τ_{AC} are the squares of concurrence Eq.12, between A and B, and A and C respectively. Consequently they defined the 3-tangle (or residual tangle)

τ_{ABC} as follows:

$$\tau_{A(BC)} = \tau_{AB} + \tau_{AC} + \tau_{ABC} \quad (15)$$

To be read, the entanglement of A with the rest of the system is equal to the entanglement of A with B alone, plus the entanglement of A with C alone plus the 3-tangle of the whole system. The 3-tangle quantify the residual three-particle entanglement, which cannot be accounted for by the pairwise entanglement. For the GHZ-state we have $1 = 0 + 0 + \tau_{ABC}$. Also they showed that the inequality (14) is true in case of three particle in a joint mixed state

On the other hand the Peres-Horodecki criterion for separability [12, 13] leads to a natural computable measure of entanglement, called negativity [14, 15, 16]. The negativity is based on the trace norm of the partial transpose ρ^{TA} of the bipartite mixed state ρ_{AB} , and measures the degree to which ρ^{TA} fails to be positive. The density matrices which represent physical systems are non-negative matrices with unit trace, the partial transpose also satisfies $\text{Tr}\{\rho^{TA}\} = 1$, but since it may have negative eigenvalues μ_i for entangled states" therefore its trace norm reads in general

$$\|\rho^{T_1}\|_1 = 1 + 2 \left| \sum_i \mu_i \right| \equiv 1 + \mathcal{N}(\rho) \quad (16)$$

where $\mathcal{N}(\rho)$ is the negativity, i.e. the absolute value of twice the sum of the negative eigenvalues. Vidal and Werner [16] proved that the negativity $\mathcal{N}(\rho)$ is an entanglement monotone and therefore it is a good measure of entanglement. Following [16], the residual three-particle entanglement \mathcal{N}_{abc} in our case can be quantified using the relation

$$\mathcal{N}_{abc} = \mathcal{N}_{a-bc}(\rho_{abc}) - \mathcal{N}_{a-b}(\rho_{ab}) - \mathcal{N}_{a-c}(\rho_{ac}) \quad (17)$$

$$\mathcal{N}_{a-bc}(\rho_{abc}) = \|\rho_{abc}^{T_a}\|_1 - 1 \quad (18)$$

$$\mathcal{N}_{a-b}(\rho_{ab}) = \|\rho_{ab}^{T_a}\|_1 - 1 \equiv \|\rho_{ab}^{T_b}\|_1 - 1 \quad (19)$$

$$\mathcal{N}_{a-c}(\rho_{ac}) = \|\rho_{ac}^{T_a}\|_1 - 1 \equiv \|\rho_{ac}^{T_c}\|_1 - 1 \quad (20)$$

The term $\mathcal{N}_{a-bc}(\rho_{abc})$ quantifies the strength of quantum correlations between the atom "a" and the other two atoms. The remaining two terms quantify the pairwise entanglement between the atom "a" and b or c. Note that the partial trace operation belongs to the set of local operations and classical communication (LOCC) under which the entanglement can not increase. Therefore the left hand side of Eq.17 is a residual three-particle entanglement. In our case $\mathcal{N}_{a-b}(\rho_{ab}) = \mathcal{N}_{a-c}(\rho_{ac})$ because of the symmetry. In Fig.4 we show the results for the different initial states. We see that the residual 3-particle entanglement changes between local maxima and minima during the evolution. The local maxima occur at

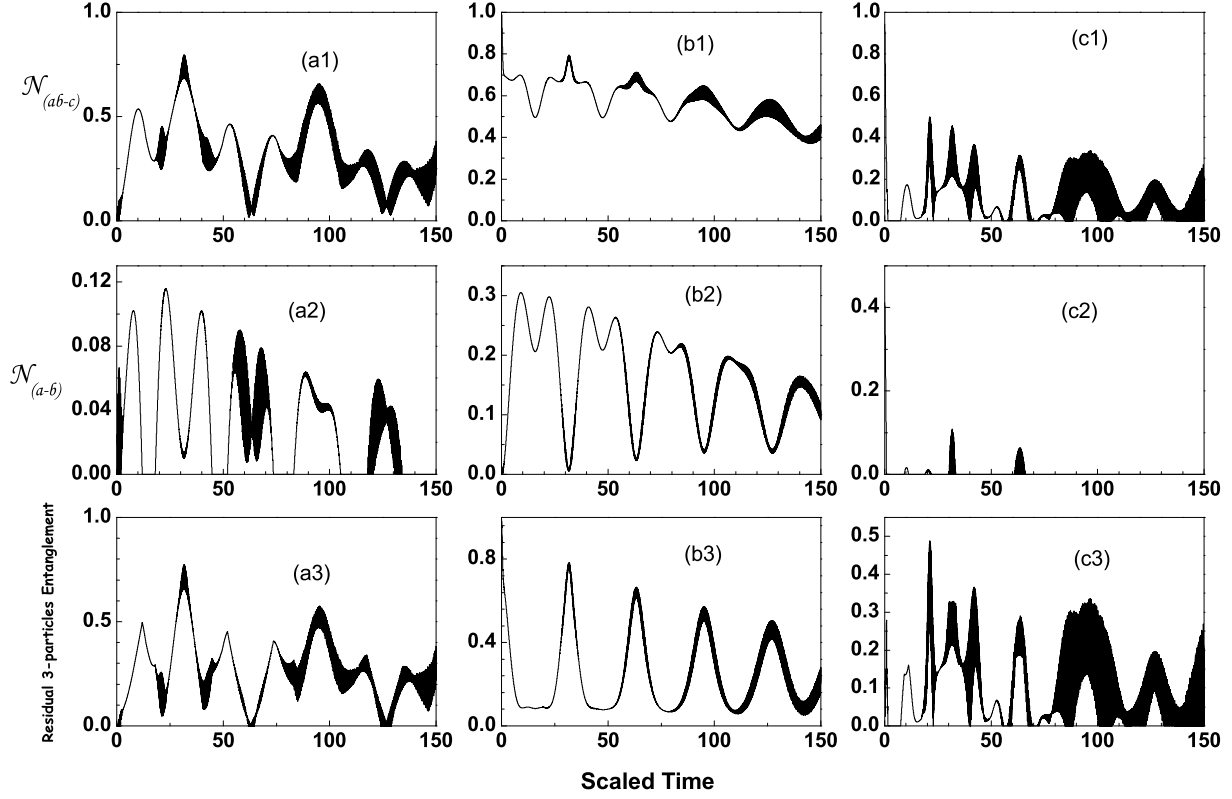


FIG. 4: Evolution of the negativity $\mathcal{N}_{a-bc}(\rho_{abc})$, $\mathcal{N}_{a-b}(\rho_{ab})$ and the residual 3-particles negativity \mathcal{N}_{abc} for different initial atomic states (a) $|eee\rangle$ -initial state, (b) $|GHZ\rangle$ -initial state and (c) $|W\rangle$ -initial state.

half-revival times, when the the atoms became most disentangled from the field. Asymptotically this residual entanglement vanishes and the atomic system becomes maximally entangled with the field. From Figs. 3 and 4 it is shown that the negativity measure of two-atom entanglement is less than or at most equal to the concurrence as it is conjectured in [15].

Q-FUNCTION

In this section we return to the entanglement between the field and the atomic system but through the field dynamic, namely we will discuss the field quasi-probability distribution function, the Q-function [50], defined as $Q(\beta, t) = \frac{1}{\pi} \langle \beta | \rho_f(t) | \beta \rangle$. By using Eq.(5) we get the following form of the Q-function in terms of probability amplitudes.

$$Q(\alpha, t) = \frac{e^{-|\beta|^2}}{\pi} \sum_{i=1}^4 \left| \sum_{n=0}^{\infty} \frac{(\beta^*)^{n+i-1}}{\sqrt{(n+i-1)!}} X_i^{(n)} \right|^2 \quad (21)$$

Figs.5,6, 7 show the Q -function for different initial atomic states at different characteristic times $t_0 = 0$, $t_1 = \frac{\pi}{3}\sqrt{\bar{n}}$, $t_2 = \frac{2\pi}{3}\sqrt{\bar{n}}$, $t_3 = \pi\sqrt{\bar{n}}$, $t_4 = \frac{4\pi}{3}\sqrt{\bar{n}}$, $t_5 = 2\pi\sqrt{\bar{n}}$. The field is initially in a coherent state with average photon number $|\alpha_0|^2 = \bar{n} = 100$. At $\tau = 0$ the shape of the Q-function is a Gaussian centered at $(\sqrt{\bar{n}}, 0)$ as expected for the initial coherent state. But as time develops we found different types of behavior associated with each initial atomic state. For the state $|eee\rangle$ depicted in Fig.5; we note that the single peak is splitted into two pairs, a pair with large amplitude moving slowly in opposite directions and the other pair of the smaller amplitudes moving fastly in opposite directions. To shed some light on this behavior, rough analysis of formula (21), similar to that used in the atomic inversion, shows that time dependent factors in the summand behave like $\{\cos 3(\sqrt{\bar{n}} - \sqrt{\bar{m}})\tau + 3 \cos(\sqrt{\bar{n}} - \sqrt{\bar{m}})\tau\}$. This form exhibits clearly the appearance of the pairs and the first term represents the faster pair while the second term represents the slower pair with amplitude 3 times larger than the faster ones. Note the appearance of the

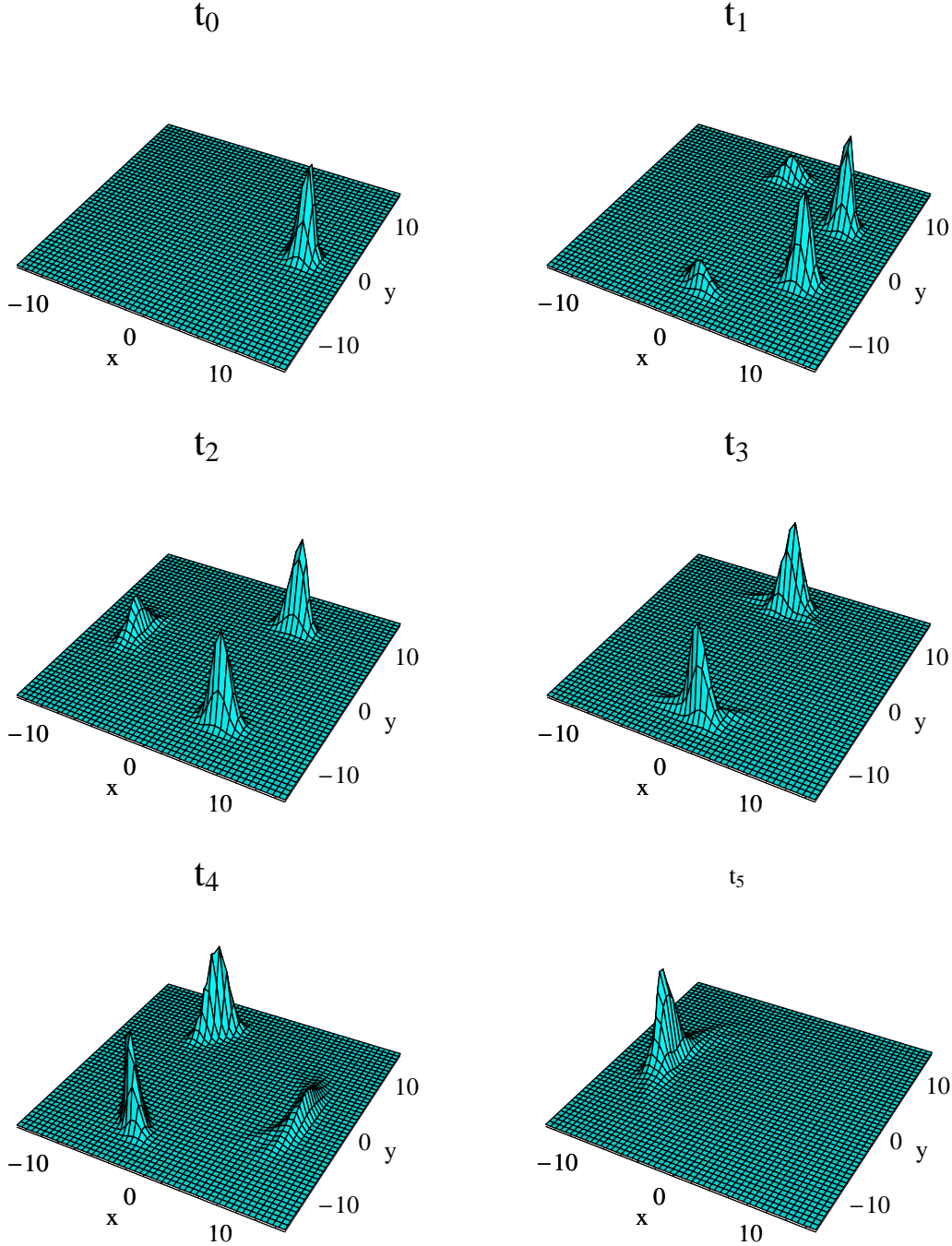


FIG. 5: The Q-function for the initial atomic state $|\Psi(0)\rangle = |eee\rangle$

Schrödinger cat-state [32], at half-revival ($\tau = t_3$). The case of the state $\frac{1}{\sqrt{2}}(|ggg\rangle + |eee\rangle)$ is quite interesting. Here the peak splits into only two peaks; a small faster peak and a large slower peak. The analysis shows that the time-dependent factor in the summand behaves as $\{e^{3i(\sqrt{m}-\sqrt{n})\tau} + 3e^{i(\sqrt{n}-\sqrt{m})\tau}\}$ which exhibits the two single peaks, they move in opposite directions and the

larger is the slower peak. The third case of the Werner state as depicted in Fig.7 shows an opposite behaviour to that of the $|eee\rangle$ state. The pair with the larger amplitude moves faster than the pair with smaller amplitude. The time dependent-factor in the summand in this case behaves like $\{3 \cos 3(\sqrt{n} - \sqrt{m})\tau + \cos(\sqrt{n} - \sqrt{m})\tau\}$ which demonstrates the fast movement of the larger

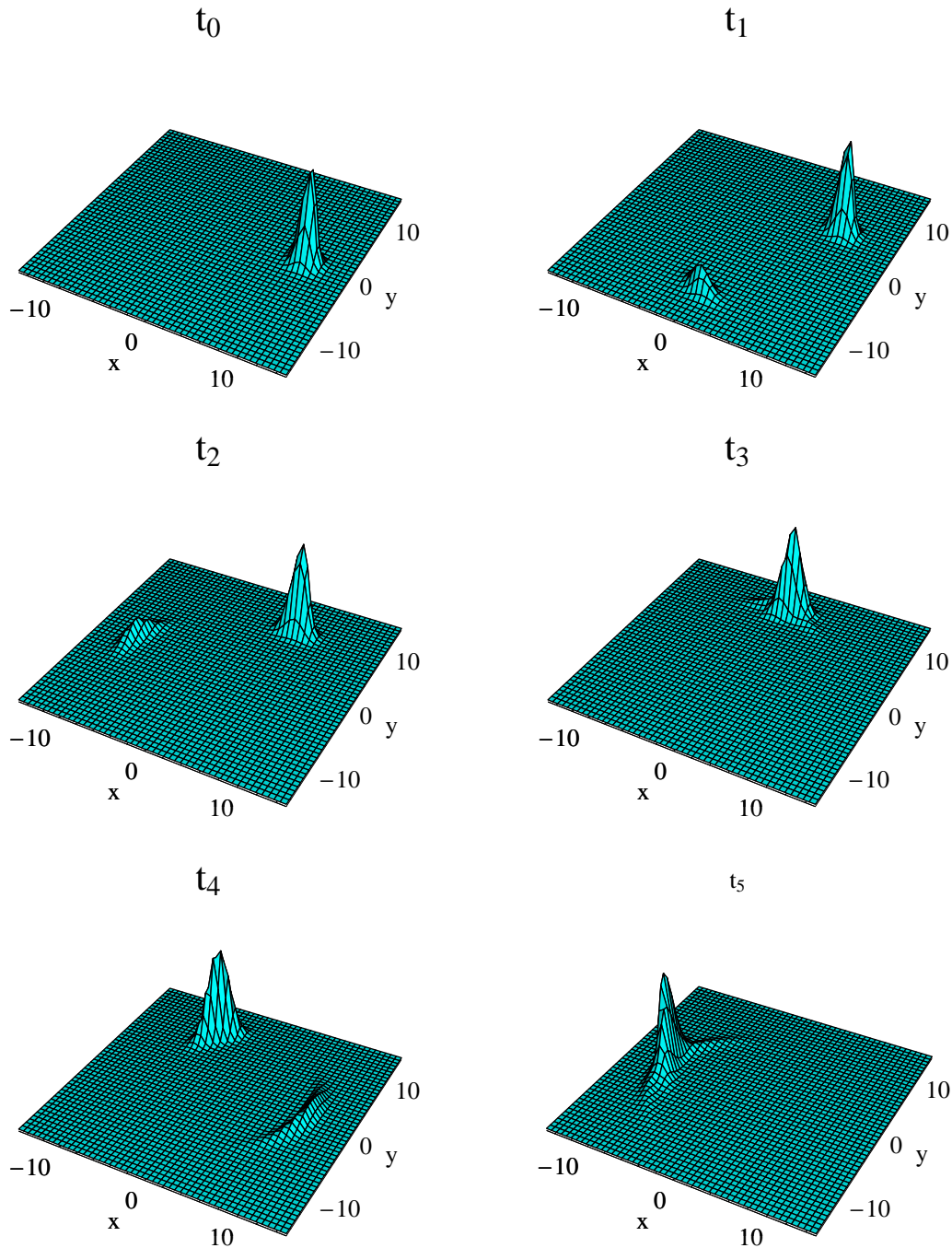


FIG. 6: The Q-function for the initial atomic state $|\Psi(0)\rangle = \frac{1}{\sqrt{2}}(|eee\rangle + |ggg\rangle)$

components and the slow movement of the smaller components. It is to be remarked that at half revival time starting from either the uppermost excited state ($|eee\rangle$) or the Werner state the Schrödinger cat-state is produced. On the other hand starting from the GHZ-state we find that at half revival time the field state returns to its original state. Because as the larger

component moves $\frac{\pi}{2}$ in the phase space the smaller and faster component would move $\frac{3\pi}{2}$ on the other direction and meets the larger one. The previous behavior is also demonstrated in Fig.1.(b) regarding the atomic inversions

Now looking at the various entanglement evolution

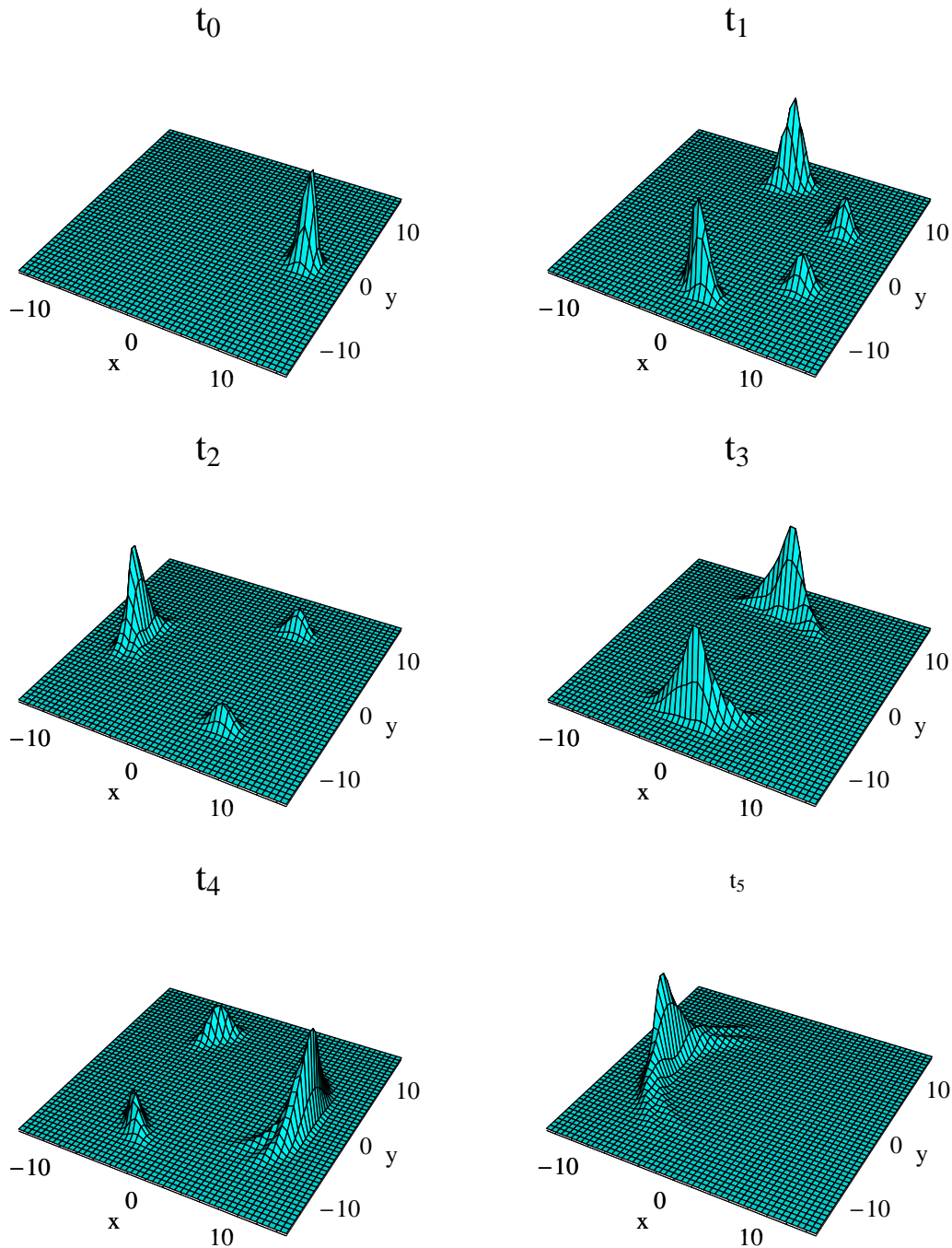


FIG. 7: The Q-function for the initial atomic state $|\Psi(0)\rangle = \frac{1}{\sqrt{3}}(|eeg\rangle + |ege\rangle + |gee\rangle)$

Figs.2 and 4 we find that there is a clear connection between the Q-function dynamic and various entanglement evolutions. For the $|eee\rangle$ and $|W\rangle$ initial states, at half the first-revival time t_1 which correspond to a local minima of I-Concurrence, $I_{f(abc)}$ in the $|eee\rangle$ case and to the minimum value in the $|W\rangle$ case, the faster peaks became most apart from each other. Also at that time the resid-

ual 3-particle entanglement has a local maximum. At the first-revival time t_3 these two peaks collide and recombine, and this corresponds to a local minima of $I_{f(abc)}$ in the two cases, a local minima of the residual 3-particle in $|eee\rangle$ case and a maximum value in the $|W\rangle$ case. Also we note that the amplitude of these two peaks increase significantly in the $|W\rangle$ case. This behavior can be con-

nected to Figs.3.(c1),(c2),(c3), where it is clear that at that time t_4 the entanglement of all the atomic ensembles with the field is minimum and this is not the case in the $|eee\rangle$ state. The last interesting feature we want to mention here for the $|eee\rangle$ and Wener cases is that, at t_5 , the Q-function, shows phase squeezing.

DISCUSSION AND CONCLUSION

In this paper we consider a system of identical three two-level atoms interacting at resonance with a single-mode of the quantized field in a lossless cavity. The initial cavity field is prepared in the coherent state while the atoms are taken in different initial states, namely the atoms taken to be in the excited state, $|eee\rangle$, the GHZ entangled state and the Wener entangled state. For this system we investigated different kinds of entanglement, atoms-field cooperative and atoms-pairwise entanglements. We use the concurrence, the generalized I-concurrence and the negativity as measures of these types of entanglements. The relationship between this entanglement and the collapse and revival in the atomic inversion is investigated. Also the Q -functions for different cases are discussed and connected to different entanglements evolutions of the system. Most noteworthy we found that the GHZ-state is more robust against energy losses, and showing almost coherent trapping. Also one can say that the entanglement of GHZ-state is more robust than the W-state. These two different behav-

iors have been distinctly shown through the study, perfectly depicted in Fig.1.(b1) and Fig.4.(b1) respectively. This suggests that the GHZ-state may show more resistance to the decoherence phenomena than any other three-partite entanglement. Consequently it may be a primary candidate for many quantum information tasks, which need a three-partite entanglement state. In fact the GHZ-state is a resource for many applications, these include, quantum secret sharing [51], open destination teleportation [52] and quantum computation [53]. On the other hand for the other two cases ($|eee\rangle$ and W states) the Schrödinger cat-state is produced. Another interesting feature is the clear link between the Q-function dynamics and various entanglement evolution. Finally we found that, while the W-state, is the state with the maximal possible bipartite entanglement in the reduced two-qubit states, its initial entanglement vanishes very rapidly. Moreover the production of such pairwise entanglement through the evolution is very small. This in contrast to the other two cases which have no pairwise entanglement initially but such entanglement increase greatly through the evolution. Sudden death and sudden revival of atoms-pairwise entanglement are produced with the W-state

APPENDIX : EVOLUTION MATRIX FOR THE PROBABILITIES AMPLITUDES

In this appendix we give the explicit form of the elements of the evolution matrix \mathcal{U} appearing in Eq.(6)

$$\begin{aligned}
\mathcal{U}_{11} &= \left[\frac{\mu_1 - 4\beta^2 - 3\eta^2}{(\mu_1 - \mu_2)} \cos(\sqrt{\mu_1} \tau) + \frac{\mu_2 - 4\beta^2 - 3\eta^2}{(\mu_2 - \mu_1)} \cos(\sqrt{\mu_2} \tau) \right] \\
\mathcal{U}_{12} &= -i\sqrt{3}\gamma \left[\frac{\mu_1 - 3\eta^2}{\sqrt{\mu_1}(\mu_1 - \mu_2)} \sin(\sqrt{\mu_1} \tau) + \frac{\mu_2 - 3\eta^2}{\sqrt{\mu_2}(\mu_2 - \mu_1)} \sin(\sqrt{\mu_2} \tau) \right] \\
\mathcal{U}_{13} &= 2\sqrt{3}\beta\gamma \left[\frac{1}{(\mu_1 - \mu_2)} \cos(\sqrt{\mu_1} \tau) + \frac{1}{(\mu_2 - \mu_1)} \cos(\sqrt{\mu_2} \tau) \right] \\
\mathcal{U}_{14} &= -6i\beta\gamma\eta \left[\frac{1}{\sqrt{\mu_1}(\mu_1 - \mu_2)} \sin(\sqrt{\mu_1} \tau) + \frac{1}{\sqrt{\mu_2}(\mu_2 - \mu_1)} \sin(\sqrt{\mu_2} \tau) \right] \\
\mathcal{U}_{22} &= \left[\frac{\mu_1 - 3\eta^2}{(\mu_1 - \mu_2)} \cos(\sqrt{\mu_1} \tau) + \frac{\mu_2 - 3\eta^2}{(\mu_2 - \mu_1)} \cos(\sqrt{\mu_2} \tau) \right] \\
\mathcal{U}_{23} &= -2i\beta \left[\frac{\sqrt{\mu_1}}{(\mu_1 - \mu_2)} \sin(\sqrt{\mu_1} \tau) + \frac{\sqrt{\mu_2}}{(\mu_2 - \mu_1)} \sin(\sqrt{\mu_2} \tau) \right] \\
\mathcal{U}_{24} &= 2\sqrt{3}\beta\eta \left[\frac{1}{(\mu_1 - \mu_2)} \cos(\sqrt{\mu_1} \tau) + \frac{1}{(\mu_2 - \mu_1)} \cos(\sqrt{\mu_2} \tau) \right] \\
\mathcal{U}_{33} &= \left[\frac{\mu_1 - 3\gamma^2}{(\mu_1 - \mu_2)} \cos(\sqrt{\mu_1} \tau) + \frac{\mu_2 - 3\gamma^2}{(\mu_2 - \mu_1)} \cos(\sqrt{\mu_2} \tau) \right] \\
\mathcal{U}_{34} &= -i\sqrt{3}\eta \left[\frac{\mu_1 - 3\gamma^2}{\sqrt{\mu_1}(\mu_1 - \mu_2)} \sin(\sqrt{\mu_1} \tau) + \frac{\mu_2 - 3\gamma^2}{\sqrt{\mu_2}(\mu_2 - \mu_1)} \sin(\sqrt{\mu_2} \tau) \right] \\
\mathcal{U}_{44} &= \left[\frac{\mu_1 - 4\beta^2 - 3\gamma^2}{(\mu_1 - \mu_2)} \cos(\sqrt{\mu_1} \tau) + \frac{\mu_2 - 4\beta^2 - 3\gamma^2}{(\mu_2 - \mu_1)} \cos(\sqrt{\mu_2} \tau) \right]
\end{aligned}$$

* Electronic address: mohamadmath@yahoo.com

- [1] A. Peres, *Quantum Theory: Concepts and Methods* (Kluwer Academic, Dordrecht, The Netherlands, 1993).
- [2] M. A. Nielsen and I. L. Chuang, *Quantum Computation and Quantum information* (Cambridge University, Cambridge, UK, 2000).
- [3] D. Deutsch, Proc. R. Soc. Lond. A **400**, 97 (1985).
- [4] C. H. Bennet, G. Brassard, C. Crépeau, R. Jozsa, A. Peres, and W. K. Wootters, Phys. Rev. Lett. **70**, 1895 (1993).
- [5] C. H. Bennet and S. Wiesner, Phys. Rev. Lett. **69**, 2881 (1992).
- [6] M. Hillery, V. Bužek, and A. Berthiaume, Phys. Rev. A. **59**, 1829 (1999).
- [7] E. T. Jaynes and F. W. Cummings, Proc. IEEE **51**, 89 (1963).
- [8] B. W. Shore and P. L. Knight, J. Mod. Opt. **40**, 1195 (1993).
- [9] S. J. D. Phoenix and P. L. Knight, Ann. Phys. **186**, 381 (1988).
- [10] J. Gea-Banacloche, Phys. Rev. Lett. **65**, 3385 (1990).
- [11] J. Gea-Banacloche, Phys. Rev. A. **44**, 5913 (1991).
- [12] A. Peres, Phys. Rev. Lett. **77**, 1413 (1996).
- [13] M. Horodecki, P. Horodecki, and R. Horodecki, Phys. Lett. A **223**, 1 (1996).
- [14] K. Zyczkowski, P. Horodecki, A. Sanpera, and M. Lewenstein, Phys. Rev. A **58**, 883 (1998).
- [15] K. Zyczkowski, Phys. Rev. A **60**, 3496 (1999).
- [16] G. Vidal and R. F. Werner, Phys. Rev. A **65**, 032314 (2002).
- [17] R. H. Dicke, Phys. Rev. **93**, 99 (1954).
- [18] M. Tavis and F. W. Cummings, Phys. Rev. **170**, 379 (1968).
- [19] M. Tavis and F. W. Cummings, Ibid. **188**, 692 (1969).
- [20] J. Kempe, Phys. Rev. A **60**, 910 (1999).
- [21] L. Pedersen and C. Rangan, Quantum Information Processing **7**, 33 (2008).
- [22] T. Monz, K. Kim, W. Hänsel, M. Riebe, A. S. Villar, P. Schindler, M. Chwalla, M. Hennrich, and R. Blatt, Phys. Rev. Lett. **102**, 040501 (2006).
- [23] A. Joshi and M. Xiao, Phys. Rev. A **74**, 052318 (2006).
- [24] S. Rai and J. Rai, arXiv:quant-ph/0006107 (2000).
- [25] I. K. Kudryavtsev, A. Lambrecht, H. Moya-Cessa, and P. L. Knight, J. Mod. Opt. **40**, 1605 (1993).
- [26] J. H. Eberly, N. B. Narozhny, and J. J. Sanchez-Mondragon, Phys. Rev. Lett. **44**, 1323 (1980).
- [27] N. B. Narozhny, J. J. Sanchez-Mondragon, and J. H. Eberly, Phys. Rev. A. **23**, 236 (1981).
- [28] H. I. Yoo, J. J. Sanchez-Mondragon, and J. H. Eberly, J. Phys. A. **14**, 1383 (1981).
- [29] H. I. Yoo and J. H. Eberly, Phy. Rep. **118**, 239 (1985).
- [30] S. J. D. Phoenix and P. L. Knight, Phys. Rev. Lett. **66**, 2833 (1991).
- [31] S. J. D. Phoenix and P. L. Knight, Phys. Rev. A. **44**, 6023 (1991).
- [32] V. Bužek, H. Moya-Cessa, P. L. Knight, and S. J. D. Phoenix, Phys. Rev. A. **45**, 8190 (1992).
- [33] W. P. Schleich, *Quantum Optics in Phase Space* (WILEY-VCH, Berlin, 2001).
- [34] W. Vogel and D.-G. Welsch, *Quantum Optics* (WILEY-VCH Verlag Berlin, Berlin, 2006).

- [35] D. M. Greenberger, M. Horne, , and A. Zeilinger, *in Bells Theorem, Quantum Theory, and Conceptions of the Universe* (Kluwer Academic, Dordrecht, The Netherlands, 1989).
- [36] W. Dur, G. Vidal, and J. I. Cirac, *Phys. Rev. A* **62**, 062314/1 (2000).
- [37] K. Zaheer and M. S. Zubairy, *Phys. Rev. A* **39**, 2000 (1989).
- [38] V. Coffman, J. Kundu, and W. K. Wootters, *Phys. Rev. A* **61**, 052306/1 (2000).
- [39] P. Rungta, V. Bužek, C. M. Caves, H. Hillery, and G. J. Milburn, *Phys. Rev. A* **64**, 042315 (2001).
- [40] S. Hill and W. K. Wootters, *Phys. Rev. Lett.* **78**, 5022 (1997).
- [41] R. Alicki and K. Lendi, *Quantum Dynamical Semigroups and Applications* (Springer, Berlin, 1987).
- [42] J. A. S. C. H. Bennett, D. P. DiVincenzo and W. K. Wootters, *Phys. Rev. A* **54**, 3824 (1996).
- [43] C. H. Bennett, H. J. B. S. Popescu, and B. Schumacher, *Phys. Rev. A* **53**, 2046 (1996).
- [44] W. K. Wootters, *Phys. Rev. Lett.* **51**, 2245 (1998).
- [45] T. J. Osborne, *Phys. Rev. A* **72**, 022309 (2005).
- [46] T. Yu and J. Eberly, *Phys. Rev. Lett.* **93**, 140404 (2004).
- [47] Z. Ficek and R. Tanas, *Phys. Rev. A* **74**, 024304 (2006).
- [48] Z. Ficek and R. Tanas, *Phys. Rev. A* **77**, 054301 (2008).
- [49] D. Xiao-Juan and F. Mao-Fa, *Chinese Physics B* **17**, 3209 (2008).
- [50] M. O. Scully and M. S. Zubairy, *Quantum Optics* (University Press, Cambridge, 1997).
- [51] M. Hillery, V. Bužek, and A. Berthiaume, *Phys. Rev. A* **59**, 1829 (1999).
- [52] Z. Zhao, Y.-A. Chen, A.-N. Zhang, T. Yang, H. Briegel, and J.-W. Pan, *Nature* **430**, 54 (2004).
- [53] D. Gottesman and I. Chuang, *Nature* **402**, 390 (1999).